

**STUDY OF SEAWATER INTRUSION AND  
CONTROLLING METHODS  
USING PHYSICAL MODEL SIMULATIONS**

**Pajeeraporn Weingchanda**

**A Thesis Submitted in Partial Fulfillment of the Requirements  
for the Degree of Master of Engineering in Geotechnolgy**

**Suranaree University of Technology**

**Academic Year 2010**

การศึกษาการรูก้าของน้ำทะเลและวิธีการควบคุม  
โดยใช้แบบจำลองเชิงกายภาพ

นางสาวพจิราภรณ์ เวียงจันดา

วิทยานิพนธ์นี้เป็นส่วนหนึ่งของการศึกษาตามหลักสูตรปริญญาวิศวกรรมศาสตรมหาบัณฑิต  
สาขาวิชาเทคโนโลยีธรณี  
มหาวิทยาลัยเทคโนโลยีสุรนารี  
ปีการศึกษา 2553

**STUDY OF SEAWATER INTRUSION AND CONTROLLING  
METHODS USING PHYSICAL MODEL SIMULATIONS**

Suranaree University of Technology has approved this thesis submitted in partial fulfillment of the requirements for a Master's Degree.

Thesis Examining Committee

---

(Asst. Prof. Thara Lekuthai)

Chairperson

---

(Assoc. Prof. Dr. Kittitep Fuenkajorn)

Member (Thesis Advisor)

---

(Dr. Prachya Tepnarong)

Member

---

(Prof. Dr. Sukit Limpijumnong)

Vice Rector for Academic Affairs

---

(Assoc. Prof. Dr. Vorapot Khompis)

Dean of Institute of Engineering

พจิราภรณ์ เวียงจันดา : การศึกษาการรุกล้ำของน้ำทะเลและวิธีการควบคุม โดยใช้  
แบบจำลองเชิงกายภาพ (STUDY OF SEAWATER INTRUSION AND CONTROLLING  
METHODS USING PHYSICAL MODEL SIMULATIONS) อาจารย์ที่ปรึกษา :  
รองศาสตราจารย์ ดร.กิตติเทพ เฟื่องขจร, 77 หน้า.

วัตถุประสงค์ของงานวิจัยนี้คือ การศึกษาการจำลองการรุกล้ำของน้ำทะเลเข้าสู่ชั้นน้ำบาดาลที่ไม่มีชั้นหินปิดทับและเพื่อทดสอบประสิทธิภาพของวิธีการแก้ไขหรือบรรเทาปัญหาการรุกล้ำของน้ำทะเลเข้าสู่ชั้นน้ำบาดาลที่ไม่มีชั้นหินปิดทับ โดยใช้แบบจำลองเชิงกายภาพที่สร้างขึ้นในห้องปฏิบัติการ วิธีการแก้ไขที่ศึกษาประกอบด้วย การสร้างแนวบ่ออัดน้ำจืด การสร้างบ่อสูบน้ำเค็มตามแนวชายฝั่ง และการสร้างแนวทึบน้ำใต้ดิน ผลที่ได้จากการทดสอบแบบสถานะตามธรรมชาติและจากการคำนวณจากความสัมพันธ์ของ Ghyben-Herzberg มีค่าสอดคล้องกัน ผลกระทบจากการสูบน้ำจะทำให้แนวรอยต่อระหว่างชั้นน้ำบาดาลและน้ำเค็มเคลื่อนตัวไปยังบ่อสูบน้ำบาดาลทำให้เกิดความเค็มที่บ่อน้ำบาดาลแต่ทั้งนี้จะขึ้นกับอัตราการสูบน้ำ ความแตกต่างระหว่างน้ำจืดและน้ำเค็มและระดับน้ำเค็มซึ่งจากการทดสอบจะพบว่าเมื่อระดับความแตกต่างระหว่างน้ำจืดและน้ำเค็มมีค่าน้อยและมีอัตราการสูบน้ำที่สูงจะส่งผลให้เกิดการปนเปื้อนน้ำเค็มที่บ่อสูบน้ำ การอัดน้ำจืดในอัตราประมาณร้อยละ 10 ของอัตราการเติมน้ำจืดจะส่งผลให้แนวรอยต่อระหว่างชั้นน้ำบาดาลและน้ำเค็มเคลื่อนตัวออกไปยังแนวชายฝั่งทะเล ส่งผลให้น้ำในบ่อสูบน้ำลดความเค็มหรือไม่มี ความเค็มเลย ความมีประสิทธิภาพของแนวทึบน้ำใต้ดินขึ้นอยู่กับความลึกของแนวทึบน้ำใต้ดินที่อยู่ใต้ระดับน้ำเค็ม โดยจากผลการทดลองพบว่าเมื่อความลึกของแนวทึบน้ำใต้ดินอยู่ที่ระดับเท่ากับระดับของน้ำเค็มจะส่งผลให้แนวทึบน้ำใต้ดินมีประสิทธิภาพมากที่สุด

สาขาวิชาเทคโนโลยีธรณี

ปีการศึกษา 2553

ลายมือชื่อนักศึกษา \_\_\_\_\_

ลายมือชื่ออาจารย์ที่ปรึกษา \_\_\_\_\_

PAJEERAPORN WEINGCHANDA : STUDY OF SEAWATER  
INTRUSION AND CONTROLLING METHODS USING PHYSICAL  
MODEL SIMULATIONS. THESIS ADVISOR : ASSOC. PROF. KITTITEP  
FUENKAJORN, Ph.D., PE., 77 PP.

SEAWATER/GROUNDWATER/INTRUSION/SALINITY/PERMEABILITY

The objectives of this research are to simulate the seawater intrusion into unconfined aquifers and to assess the efficiency of the controlling methods by using scaled-down physical models. The controlling methods to be studied here include injection barrier, extraction wells, and subsurface barrier. Physical scaled-down model has been used to simulate salt water intrusion into unconfined aquifer near shoreline. The results indicate that under natural dynamic equilibrium between the recharge of fresh water and salt water intrusion the salinity measurements agree reasonably well with the solution given by Ghyben-Herzberg. Fresh water pumping (usage) notably move the fresh-salt water interface toward the well, depending on the pumping rates and the difference between the far-field discharge (fresh water reservoir) and salt water level ( $\Delta h$ ). Fresh water injection near the shoreline is more favorable than salt water extraction. The fresh water injection rate of about 10% of the discharge rate at the well can effectively push the interface toward the shoreline, and keeping the pumping water free of salinity. The effectiveness of subsurface barrier technique depends heavily on the depth of the barrier below the salt water level. The optimum barrier depth of the barrier is equivalent to  $\Delta h$  which can effectively press the interface below the depth of the pumping well.

School of Geotechnology

Academic Year 2010

Student's Signature \_\_\_\_\_

Advisor's Signature \_\_\_\_\_

## **ACKNOWLEDGEMENTS**

The author wishes to acknowledge the support from the Suranaree University of Technology (SUT) who provided funding for this research.

Grateful thanks and appreciation are given to Assoc. Prof. Dr. Kittitep Fuenkajorn, thesis advisor, who lets the author work independently, but gave a critical review of this research. Many thanks are also extended to Asst. Prof. Thara Lekuthai and Dr. Prachaya Tepnarong, who served on the thesis committee and commented on the manuscript.

Finally, I most gratefully acknowledge my parents and friends for all their supported throughout the period of this research.

Pajeeraporn Weingchanda

# TABLE OF CONTENTS

	<b>Page</b>
ABSTRACT (THAI) .....	I
ABSTRACT (ENGLISH).....	II
ACKNOWLEDGEMENTS .....	IV
TABLE OF CONTENTS.....	V
LIST OF TABLES .....	VIII
LIST OF FIGURES .....	IX
LIST OF SYMBOLS AND ABBREVIATIONS .....	XII
<b>CHAPTER</b>	
<b>I INTRODUCTION.....</b>	<b>1</b>
1.1 Background of problems and significance of the study .....	1
1.2 Research objectives .....	2
1.3 Research methodology .....	2
1.4 Scope and limitations.....	4
1.5 Thesis contents .....	5
<b>II LITERATURE REVIEW .....</b>	<b>6</b>
2.1 Introduction .....	6
2.2 Literature review.....	6
2.3 Case studies .....	11

## TABLE OF CONTENTS (Continued)

	<b>Page</b>
<b>III TEST FRAME</b> .....	19
3.1 Introduction .....	19
3.2 Design of test frame .....	19
3.3 Testing materials and layout.....	19
<b>IV LABORATORY EXPERIMENTS</b> .....	25
4.1 Introduction .....	25
4.2 Test method .....	25
4.3 Test results.....	27
4.3.1 Results under natural condition .....	28
4.3.2 Simulation of water pumping effect.....	31
4.3.3 Results of the injection of fresh water .....	32
4.3.4 Results of the extraction of salt water.....	35
4.3.5 Results of the subsurface barrier.....	42
<b>V DYE TESTING</b> .....	53
5.1 Objective.....	53
5.2 Test methods.....	53
5.3 Results for natural condition.....	53
5.4 Results for water pumping .....	56
5.5 Results for injection of fresh water.....	56

**TABLE OF CONTENTS (Continued)**

	<b>Page</b>
5.6 Results for extraction of salt water .....	56
5.7 Results for subsurface barrier .....	57
<b>VI DISCUSSIONS AND CONCLUSIONS</b> .....	<b>62</b>
6.1 Discussions and conclusions .....	62
6.2 Recommendations for future studies .....	63
REFERENCES .....	64
APPENDIX	
APPENDIX A. TECHNICAL PUBLICATION .....	67
BIOGRAPHY .....	77

## LIST OF TABLES

<b>Table</b>	<b>Page</b>
4.1 Test parameter.....	28
4.2 Results of water pumping .....	32
4.3 Results of fresh water injection.....	35
4.4 Results of salt water extraction .....	42
4.5 Results of subsurface barrier.....	43

## LIST OF FIGURES

Figure	Page
1.1 Research methodology .....	3
2.1 Hydrostatic balance between fresh water and saline water illustrated by a U-tube .....	8
2.2 Idealized sketch of occurrence of fresh and saline groundwater In and unconfined coastal aquifer .....	10
2.3 Vertical cross section showing flow patterns of fresh and saline water In an unconfined coastal aquifer .....	12
2.4 Saltwater-freshwater interfaces in a confined coastal aquifer under conditions of steady state seaward flow .....	12
3.1 Perspective view of the test frame .....	20
3.2 Components of the test frame component .....	21
3.3 Top view of test frame .....	22
3.4 Side view of test frame .....	23
3.5 Test parameters and locations of monitoring point on Acrylic sheets .....	24
4.1 Show the test arrangement .....	26
4.2 Test parameters and locations of monitoring points on acrylic sheet .....	29
4.3 Flow pattern of fresh water in an unconfined coastal aquifer .....	31

## LIST OF FIGURES (Continued)

Figure	Page
4.4	Simulation under natural condition and comparison with the Ghyben-Herzberg solution at $\Delta h = 10$ cm .....33
4.5	Simulation under natural condition and comparison with the Ghyben-Herzberg solution at $\Delta h = 5$ cm.....34
4.6	Simulation of water pumping at $\Delta h = 10$ cm, $Q_{FR} = 0.2$ cc/min.....36
4.7	Simulation of water pumping at $\Delta h = 10$ cm, $Q_{FR} = 10$ cc/min.....37
4.8	Simulation of water pumping at $\Delta h = 10$ cm, $Q_{FR} = 100$ cc/min.....38
4.9	Simulation of water pumping at $\Delta h = 5$ cm, $Q_{FR} = 5$ cc/min.....39
4.10	Simulation of water pumping at $\Delta h = 5$ cm, $Q_{FR} = 30$ cc/min.....40
4.11	Simulation of water pumping at $\Delta h = 5$ cm, $Q_{FR} = 70$ cc/min.....41
4.12	Simulation of fresh water injection at MSL, $Q_{IN} = 7$ cc/min.....44
4.13	Simulation of fresh water injection at MSL, $Q_{IN} = 15$ cc/min.....45
4.14	Simulation of fresh water injection at MSL, $Q_{IN} = 50$ cc/min .....46
4.15	Simulation of salt water extraction at $-10$ cm, $Q_{SE} = 15$ cc/min .....47
4.16	Simulation of salt water extraction at $-10$ cm, $Q_{SE} = 50$ cc/min .....48
4.17	Simulation of salt water extraction at $-10$ cm, $Q_{SE} = 100$ cc/min .....49
4.18	Simulation of at subsurface barrier at $D_B = -5$ cm .....50
4.19	Simulation of at subsurface barrier at $D_B = -10$ cm .....51
4.20	Simulation of at subsurface barrier at $D_B = -15$ cm .....52

**LIST OF FIGURES (Continued)**

<b>Figure</b>	<b>Page</b>
5.1 Dye testing under natural condition at $\Delta h = 10$ cm.....	54
5.2 Dye testing under natural condition at $\Delta h = 5$ cm.....	55
5.3 Dye testing for water pumping with $\Delta h = 5$ cm with $Q_{FR} = 70$ cc/min .....	58
5.4 Dye testing for fresh water injection at MSL with $Q_{IN} = 50$ cc/min.....	59
5.5 Dye testing for salt water extraction at $- 10$ cm (10 cm below MSL) with $Q_{SE} = 50$ cc/min.....	60
5.6 Dye testing for subsurface barrier at $D_B = - 10$ cm (10 cm below MSL).....	61

## LIST OF SYMBOLS AND ABBREVIATIONS

$\rho$	=	Density of fresh water
$\rho_s$	=	Density of the saline water
$\Delta\rho$	=	Difference of the density of the saline water with fresh water
$K$	=	the hydraulic conductivity of the aquifer
$q$	=	the fresh water flow per unit length of shoreline
$x_o$	=	the width of the submarine zone through which fresh water discharges into the sea
$Z_o$	=	the depth of the interface beneath the shoreline
$Z$	=	Distance from mean sea level to interface

# CHAPTER I

## INTRODUCTION

### 1.1 Background of problems and significance of the study

Seawater intrusion or encroachment is shoreward movement of salt water from ocean into coastal aquifers due to the overpumping of groundwater, and it is a dynamic equilibrium of ground water movement. In coastal regions, successive pumping will also cause seawater intrusion, consequently leading to the possibility of polluting the groundwater and corroding subsurface structures. Fresh water and sea water are treated as two immiscible fluids; they are separated by an interface with a slope. (Fang, 1997)

When the groundwater is pumped from aquifers that are in hydraulic connection with the sea, the gradients that are set up may induce a flow of seawater from the sea toward the well. This migration of salt water into freshwater aquifers under the influence of groundwater development is known as seawater intrusion. (Freeze and Cherry, 1979)

The fresh-seawater interface however can move inland when the equilibrium system is changed (change of flow rate or change of aquifer and seawater level). The problem of seawater intrusion occurs in many countries and cities located on near-shore aquifers. This problem has increased as the population increases, the growth of industry and the increase of sea levels caused by global warming also contribute to the seawater intrusion problem.

## **1.2 Research objectives**

The objective of this research is to assess the effectiveness of methods for controlling seawater intrusion in unconfined aquifers by using physical models constructed in the laboratory. The controlling methods in this study include; extraction of salt water, injection of fresh water and subsurface barrier.

The results of this research not only several the efficiency of each method but also improve our understanding of the seawater intrusion into aquifer. Accuracy and reliability Ghyben-Herzberg relation will be verified.

## **1.3 Research methodology**

As shown in Figure 1.1, this research divided is 6 steps; including literature review, design of schemes testing, laboratory testing, numerical model, analysis, discussion and conclusion.

### **1.3.1 Literature review**

Literature review will be carried out to improve an understanding of seawater intrusion knowledge. The sources of information are from journals, technical reports, and conference papers. A summary of the literature review will be given in the thesis.

### **1.3.2 Design of test frame**

The test platform for physical model test will be constructed in Geomechanical Laboratory in Suranaree University of Technology. The testing area is about 1.6m×1.2 m.

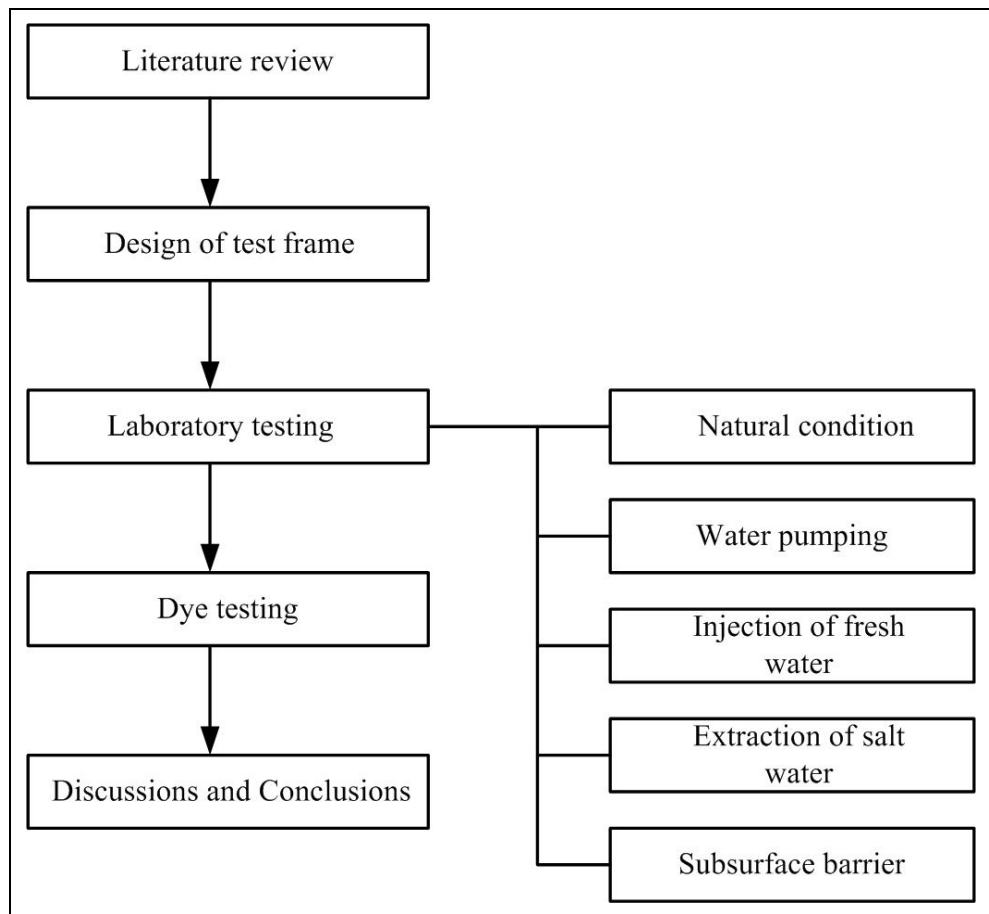


**Figure 1.1** Research Methodology

### 1.3.3 Laboratory testing

The controlling methods in this study by using physical model in laboratory include 3 types; injection of fresh water, extraction of salt water and subsurface barrier. The conditions of natural state and water pumping will be simulated.

### 1.3.4 Dye testing

The tests are performed to allow a visual inspection of the fresh and salt water interface as affected by water pumping and by the effectiveness of the three controlling methods.

### **1.3.5 Analysis**

Results from laboratory measurements in terms of seawater intrusion will be compared with Ghyben-Herzberg relation.

### **1.3.6 Discussions and Conclusions**

All research activities, methods, and results will be documented and compiled in the thesis. The research or findings will be published in the conference proceedings or journals.

## **1.4 Scope and limitations of the study**

1. Two-dimensional physical model will be used to represent the vertical cross sections in of unconfined aquifer and seawater. The area of physical model is 1.6m x 1.6m.
2. The performance of the three controlling methods for seawater intrusion will be studied.
3. Mathematical relation will be derived in terms of depth of seawater, groundwater level, rate of groundwater pumping, rate of seawater pumping and seawater level.
4. All tests will be conducted under ambient temperature.
5. Sorting sand will be used to represent model of unconfined aquifer, pure saltwater will be used to prepare the seawater.
6. A steel rod will be used to represent subsurface barrier.
7. The change of salinity in groundwater as affected by these factors will be monitored. The test will be monitored as a function of time.

## **1.5 Thesis contents**

Chapter I introduces the thesis by briefly describing the background of problems and significance of the study. The research objectives, methodology, scope and limitations are identified. Chapter II summarizes results of the literature review. Chapter III describes the physical model. Chapter IV describes the test method and presents the results obtained from the laboratory testing. Chapter V presents the dye testing results. Chapter VI concludes the research results and provides recommendations for future research studies.

## CHAPTER II

### LITERATURE REVIEW

#### 2.1 Introduction

This chapter summarizes the results of literature review carried out to improve an understanding of seawater intrusion using physical model. The topics reviewed here include the study of seawater intrusion, problem of seawater intrusion in many cities, controlling methods and problem solution.

#### 2.2 Background

More than 100 years ago two groups of investigators, working independently along the European coast, found that seawater occurred underground, not at sea level but at a depth below sea level of about 40 times the height of the fresh water above sea level. This distribution was attributed to a hydrostatic equilibrium existing between the two fluids of different densities. The equation derived to explain the phenomenon is generally referred to as the Ghyben-Herzberg relation, after its originators.

The hydrostatic balance between fresh and saline water can be illustrated by the U-tube shown in Figure 2.1 pressures on each side of the tube must be equal; therefore,

$$\rho_s g z_s = \rho_f g (z + h_f) \quad (2.1)$$

where  $\rho_s$  is the density of the saline water,  $\rho_f$  is the density of the fresh water,  $g$  is the acceleration of gravity, and  $z$  and  $h_f$  are as shown in Figure 2.1 Solving for  $z$  yields

$$z_s = \frac{\rho_f}{\rho_s - \rho_f} h_f \quad (2.2)$$

which is the Ghyben-Herzberg relation for typical seawater conditions, let  $\rho_s = 1.025$  g/cm<sup>3</sup> and  $\rho_f = 1.000$  g/cm<sup>3</sup>, so that

$$z = 40h_f \quad (2.3)$$

Translating the U-tube to a coastal situation, as shown in Figure 2.2,  $h_f$  becomes the elevation of the water table above sea level and  $z$  is the depth to the fresh-saline interface below sea level. This is a hydrodynamic rather than a hydrostatic balance because fresh water is flowing toward the sea. From density considerations alone, without flow, a horizontal interface would develop with fresh water everywhere floating above saline water. Where the flow is nearly horizontal, the Ghyben-Herzberg relation gives satisfactory results. Only near the shoreline, where vertical flow components become pronounced (see Figure 2.2) do significant errors in the position of the interface occur (Todd and Mays, 2005).

In most real situations, the Ghyben-Herzberg relation underestimates the depth to the seawater interface. Where freshwater flow to the sea takes place, the hydrostatic assumptions of the Ghyben-Herberg analysis are not satisfied.

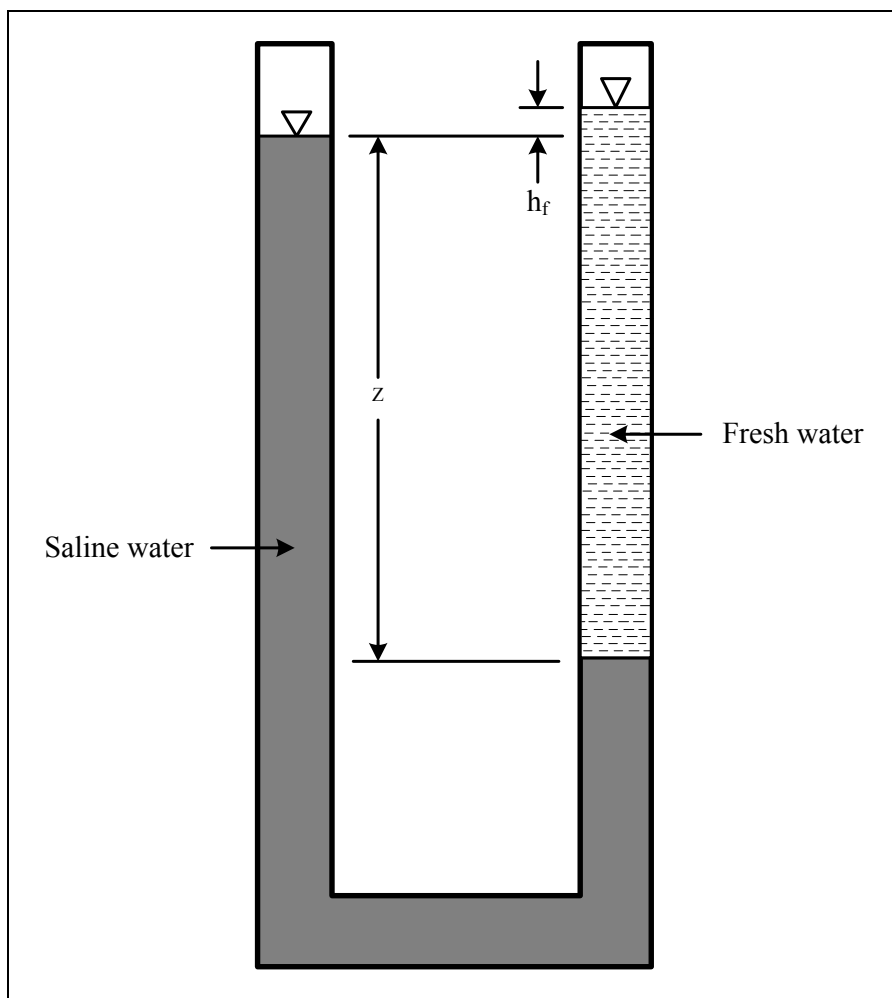


**Figure 2.1** Hydrostatic balance between fresh water and saline water illustrated by a U- tube. (Todd and Mays, 2005)

A more realistic picture was provided by Hubbert (1940) in the form of Figure 2.2 for steady-state outflow to the sea. The exact position of the interface can be determined for any given water-table configuration by graphical flow-net construction, noting the relationships shown on Figure 2.2 for the intersection of equipotential lines on the water table and on the interface.

The concepts outlined in Figures 2.1 and 2.2 do not reflect reality in yet another way. Both the hydrostatic analysis and the steady-state analysis assume that

the interface separating fresh water and salt water in a coastal aquifer is a sharp boundary. In reality, there tends to be a mixing of salt water and fresh water in a zone of diffusion around the interface. The size of the zone is controlled by the dispersive characteristics of the geologic strata. Where this zone is narrow, the methods of solution for a sharp interface may provide a satisfactory prediction of the freshwater flow pattern, but an extensive zone of diffusion can alter the flow pattern and the position of the interface, and must be taken into account. Henry (1960) was the first to present a mathematical solution for the steady-state case that includes consideration of dispersion. Cooper et al. (1964) provide a summary of the various analytical solutions.

Seawater intrusion can be induced in both unconfined and confined aquifers. Figure 2.3 provides a schematic representation of the saltwater wedge that would exist in a confined aquifer under conditions of natural steady-state outflow. Initiation of pumping (Figure 2.4) sets up a transient flow pattern that leads to declines in the potentiometric surface on the confined aquifer and inland migration of the seawater interface. Pinder and Cooper (1970) presented a numerical mathematical method for the calculation of the transient position of the saltwater front in a confined aquifer. Their solution includes consideration of dispersion.

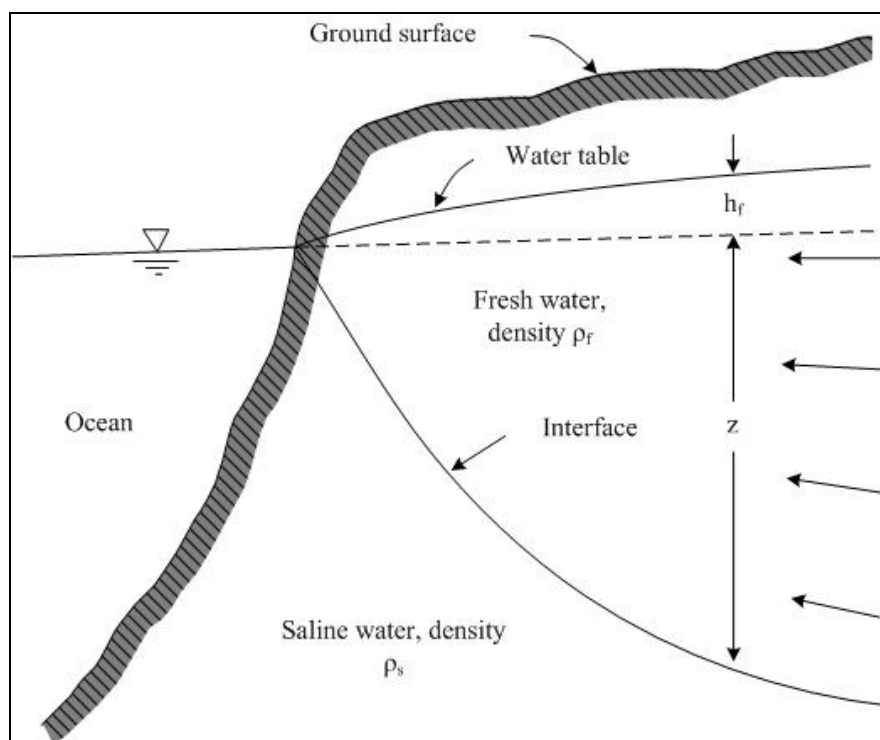


**Figure 2.2** Idealized sketch of occurrence of fresh and saline groundwater in and unconfined coastal aquifer (Todd and Mays, 2005).

One of the most intensively studied coastal aquifers in North America is the Biscayne aquifer of southeastern Florida (Kohout, 1960a; Kohout, 1960b). It is an unconfined aquifer of limestone and calcareous sandstone extending to an average depth of 30 m below sea level. Field data indicate that the seawater front undergoes transient changes in position under the influence of seasonal recharge patterns and the resulting water-table fluctuations. Lee and Cheng (1974) and Segol and Pinder (1976) have simulated transient conditions in the Biscayne aquifer with finite-element numerical models. Both the field evidence and the numerical modeling confirm the necessity of considering dispersion in the steady-state and transient analyses (Freeze and Cherry, 1979).

An important consequence of the transition zone and its seaward flow is the transport of saline water to the sea. This water originates from the underlying saline water; hence, from continuity considerations, there must exist a small landward flow in the saline water region. Figure 2.2 illustrates the flow patterns in the three subsurface zones. Field measurements at Miami and experimental studies have confirmed the landward movement of the saline water body. Where tidal action is the predominant mixing mechanism, fluctuations of groundwater and hence the thickness of the transition zone become greatest near the shoreline.

### **2.3 Case studies**

Elhassadi (2007) states that the city of Derna, Libya, located on the Green Mountain Coastal region is facing a severe water shortage problem as its water resources are exposed to sea water intrusion. This threatening phenomenon is being recurrent with several cities in the coast. This paper considers the evaluation of this problem and suggests proper means to resolve it, such as desalination.

Demirel (2003) describes the Mersin–Kazanli region as a densely industrialized region. The factories and towns cover their water demand from groundwater. With the increased water demand, saltwater intrusion has occurred. The chloride concentration of the water samples from some wells has been analysed periodically since these wells were drilled. The results of these analyses and electrical conductivity measurements were used to show the history and development of saltwater intrusion up to the year 2000. The  $\text{Cl}_2$  concentration of the water within the alluvial aquifer increased to over 3000 mg/l in 1999 and the wells were closed completely. In 2001 new wells were drilled more than 1km away from the sea and old well field. With the results of the

analyses conducted in 2001, the current groundwater quality was determined. The ground water is of the magnesium–calcium–bicarbonate type and this composition is controlled by the interaction of the water with the sediments of alluvial deposits.

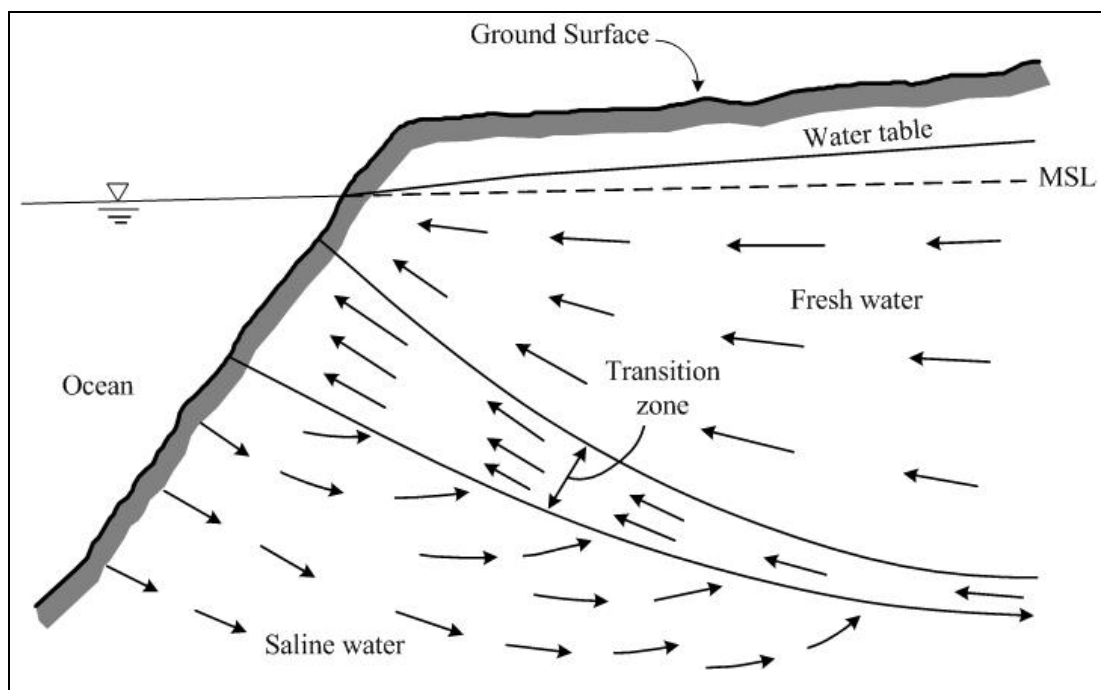


**Figure 2.3** Vertical cross section showing flow patterns of fresh and saline water in an unconfined coastal aquifer (Todd and Mays, 2005).

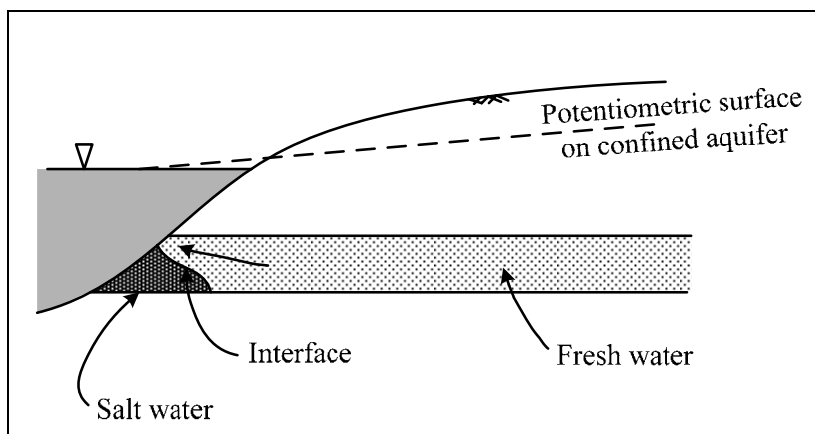


**Figure 2.4** Saltwater-freshwater interfaces in a confined coastal aquifer under conditions of steady-state seaward flow (Freeze and Cherry, 1979).

Narayan et al. (2007) study the Burdekin Delta is a major irrigation area situated in the dry tropics of North Queensland. It is unique in that (i) it overlies shallow groundwater systems that serve as a major water supply for the irrigation of sugarcane, and (ii) it is adjacent to the world heritage listed Great Barrier Reef. Water management practices include large recharge pits and surface spreading of water to assist with replenishment of the groundwater. This has been useful in maintaining groundwater levels to help control seawater intrusion. This technique, however, can be costly and ineffective in unconfined aquifer systems, which are subjected to large amounts of groundwater pumping for irrigation. There are more than 1800 production bores currently used for irrigation in the Burdekin Delta and the large volumes of water extracted have at times lowered the regional water tables and made it difficult to control seawater intrusion. In this paper we describe the use of a variable density flow and solute transport model, SUTRA, to define the current and potential extent of seawater intrusion in the Burdekin Delta under various pumping and recharge

conditions. A 2D vertical cross-section model, which accounts for groundwater pumping and recharge, was developed for the area. The Burdekin Delta aquifer consists mainly of sand and clay lenses with granitic bedrock. The model domain uses vertical cross-sections along the direction of groundwater flow. The initial conditions used in the model are based on land use prior to agricultural development when the seawater wedge was in its assumed natural state. Results of this study demonstrate the effects of variations in pumping and net recharge rates on the dynamics of seawater intrusion. Simulations have been carried out for a range of recharge, pumping rates and hydraulic conductivity values. Modeling results show that seawater intrusion is far more sensitive to pumping rates and recharge than to aquifer properties such as hydraulic conductivity. Analysis also shows that the effect of tidal fluctuations on groundwater levels is limited to areas very close to the coast. Tidal influences on saltwater intrusion therefore can be neglected when compared with the effects due to groundwater pumping. The impacts of various management options on groundwater quality are also discussed.

Giambastiani et al. (2007) study the Ravenna pine forests represent an historical landmark in the Po River Plain. They have great environmental, historical and tourist value. The San Vitale pine forest is located 10km north of the town. It is surrounded by an urban area, the city industrial infrastructure and the waterworks of the agricultural drainage system. Most land in this area is below mean sea level. As a result, no natural freshwater hydraulic gradient contrasts the density gradient of saltwater. In the last century, many events (land subsidence; land reclamation and drainage; urban and industrial development and gas and deep groundwater extractions; coastal dune destruction) led to the intrusion of large volumes of brackish and saline

groundwater. Today the freshwater in this coastal aquifer consists of low salinity water lenses floating on the saltwater wedge. This study is aimed at understanding how past and present human activities have affected the saltwater intrusion process in the phreatic aquifer and how the predicted future sea level rise will affect the salinisation process. We used a numerical model to quantify these effects on the density-dependent groundwater flow, hydraulic head and salinity distribution, seepage and salt load fluxes to the surface water system. The simulations show that over the last century artificial subsidence and heavy drainage started the salinisation process in the study area and a relative sea level rise will accelerate the increase in salt load in the coming decades, affecting the entire aquifer. Climatic conditions in the area result in limited precipitations throughout the year and preclude efficient aquifer recharge, especially in spring and summer when saltwater seepage is extensive. The lack of a continuous coastal dune system favors salt wedge intrusion.

Kouzana et al. (2007) established that intensive agricultural activities, usually, increase the risk of groundwater quality degradation through high groundwater pumping rates. In fact, the uncontrolled groundwater extraction causes a modification of natural flow systems and induces seawater intrusion from the coast and causes the groundwater quality deterioration. The Korba aquifer is located in the North-East of Tunisia, where a semi-arid Mediterranean climate prevails. The dry season is pronounced and this aggravates the situation, given that the highest water demand usually coincides with the drought period (dry weather conditions). The principal aim of this study is to characterize the hydrochemistry of this coastal aquifer, identifying the main processes that occur in the system, and to determine the extent of marine intrusion in the aquifer. In order to achieve this aim, geophysical and chemical

parameters were measured, such as vertical electrical soundings (VES), electrical conductivity, pH, temperature, anions and cations concentrations. The analytical results obtained in the hydrochemistry study were interpreted using ion correlations with chloride and  $\text{SO}_4^{2-}/\text{Cl}^-$  and  $\text{Mg}^{2+}/\text{Ca}^{2+}$  ratios, in conjunction with calculations of the ionic deviations and the saturation indexes. Saturation indexes are calculated with the PHREEQC 2.8 software used for mineral saturation modeling of the aquifer seawater-freshwater mixture. The high groundwater salinity anomaly observed in Diar El Hajjej, Garaet Sassi and Takelsa-Korba zones was explained by the presence of seawater intrusion in these areas. This hypothesis is based on high chloride concentrations, the inverse cation exchange reactions, and the lower piezometric level compared to sea level.

Milnes and Renard (2003) present coastal aquifers which are exploited for agricultural purposes. Salinisation by salt recycling from irrigation is superimposed on the effects of seawater intrusion. Water quality degradation of irrigation pumping wells caused by seawater intrusion further enhances salinisation by irrigation, as the extracted solute mass is recycled and is not withdrawn from the system. The main objective of this study is the investigation and quantification of the impact of solute recycling from irrigation relative to seawater intrusion. A solute mass budget was established by expressing the solute mass return flow as fraction of the extracted solute mass from wells by means of a solute mass return flow ratio ( $r_r$ ): The obtained expression for the relative contribution of solute recycling from irrigation is an exponential function of the return flow ratio  $r_r$  and normalised time  $t$  only (time versus system turnover time). This expression was applied to an example, the Kiti aquifer (Southern Cyprus), where field observations suggest that solute return flow is a super-

imposed salinisation mechanism. The contribution from solute recycling normalised with the solute mass flux entering from the sea after 20 years was found to be 1.5–8.5% in the extracted solute mass flux, depending on the estimation of the system turnover time. Subsequently, a coupled finite element model, reflecting the main features of the Kiti aquifer was used as a possible ‘synthetic reality’, to test the relative impact of solute recycling on the spatial salinity distribution in a complex hydrogeological and geometrical setting. This was done by running two simulation scenarios: (1) recycling all the extracted solute back into the system and (2) leaving solute recycling aside and comparing the results of these two scenarios relative to each other and to patterns observed in the field. The results showed, that by introducing solute recycling into the numerical model as coupled boundary condition does not only respect the overall solute mass balance but can have an important impact on the salinity distribution, leading to a significant spreading of the mixing zone, similar to what was observed in the field.

Nguyen et al. (2007) state that the fresh water discharges is an important parameter for modeling salt intrusion in an estuary. In alluvial converging estuaries during periods of low flow, when salinity is highest, the river discharge is generally small compared to the tidal flow. This makes the determination of the fresh water discharge a challenging task. Even if discharge observations are available during a full tidal cycle, the fresh water discharge is seldom much larger than the measurement error in the tidal discharge. Observations further upstream, outside the tidal region, do not always reflect the actual flow in the saline area due to withdrawals or additional drainage. Discharge computation is even more difficult in a complex system such as the Mekong Delta, which is a multi-channel estuary consisting of many branches, over

which the freshwater discharge distribution cannot be measured directly. This paper presents a new approach to determine the freshwater discharge distribution over the branches of the Mekong Delta by means of an analytical salt intrusion model, based on measurements made during the dry season of 2005 and 2006. It appears that the analytical model agrees well with observations and with a hydraulic model. This paper demonstrates that with relatively simple and appropriate salinity measurements and making use of the analytical salt intrusion model, it is possible to obtain an accurate discharge distribution over the branches of a complex estuary system. This makes the analytical model a powerful tool to analyze the water resources in tidal regions.

Lookjan, A., et al. (2009) study the chloride concentration of groundwater from Hat Yai aquifer, the major aquifer in the Hat Yai basin, was higher than groundwater standard. A three-dimensional density-dependent seawater intrusion model was developed for the Hat Yai basin in order to evaluate seawater intrusion from the Songkhla Lake and the Gulf of Thailand and to predicted the effect of future increase of groundwater withdrawal in the next 20 years. SEAWAT-2000 with density-dependent groundwater flow and mass transport capability was used for modeling. The developed model was calibrated using hydraulic heads and chloride concentrations from 47 observation wells. Simulation results show that for the Hat Yai basin which having annual groundwater abstraction rate of about 25 million cubic meter per year, when the abstraction rate was increased 5% annually for the next 20 years, average groundwater drawdown of 2 meters was 2 meters was observed. Particularly, for Hat Yai city, groundwater drawdown was about 3.5-10 meter. In additions, seawater intrusion area was widely apread toward Hat Yai basin.

## **CHAPTER III**

### **TEST FRAME**

#### **3.1 Introduction**

This chapter describes the design and development of the test frame used for saltwater intrusion simulation. It is designed to simulate two-dimensional flow of fresh and salt water along shorelines and to assess the performance of the controlling methods. All tests are performed in the laboratory under ambient temperature.

#### **3.2 Design of test frame**

A test frame is constructed in Geomechanics Laboratory at Suranaree University of Technology. It is developed to represent a vertical cross section of unconfined aquifer along shoreline. To allow visual inspection during the test two 1.6 m×1.2 m wide with 1.5 cm thick acrylic plates are secured in vertical position. This provides the testing area of about 1 square-meter. They are set 1.2 cm apart using steel frames. The left, right and bottom edges are sealed with rubber plates with water-tight silicone. Figures 3.1 through 3.4 show specifications and dimensions of the test frame.

#### **3.3 Testing materials and layout**

To simulate the unconfined aquifer along the shoreline the gap between the two acrylic plates is filled with sorted sand. The grain size is between 0.6-0.8 cm.

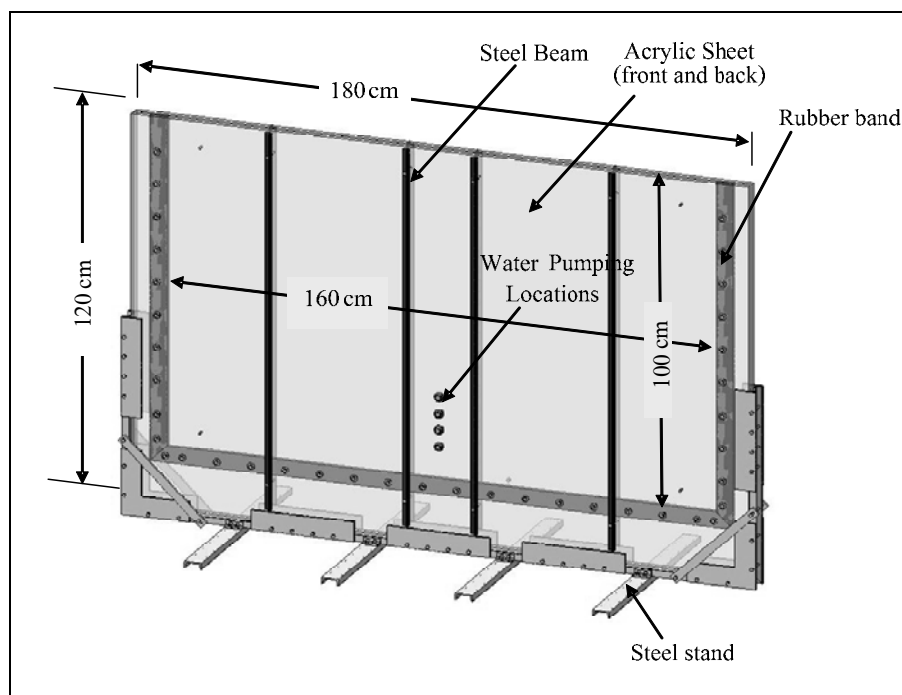


**Figure 3.1** Perspective view of the test frame.

The left side of the test frame is vertically blocked out using a strip of perforated rubber band to store fresh water supplying the water in the sand aquifer

Normally the head of the freshwater is maintained constant during each test series using external reservoir on the top of the test frame. On the right side of the test frame a perforated rubber band is used to form a shoreline with an angle of 45 degrees. The fresh and salt water can freely flow through this perforated rubber. Saturated brine is filled in the space beyond the shoreline to the right to simulate the sea. The saturated brine is continuously supplied from the top of the steel frame to maintain a constant head of the sea level. The brine is prepared by previously mixing fresh water with pure sodium chloride. Figure 3.5 shows the schematic diagram of the test layout described above

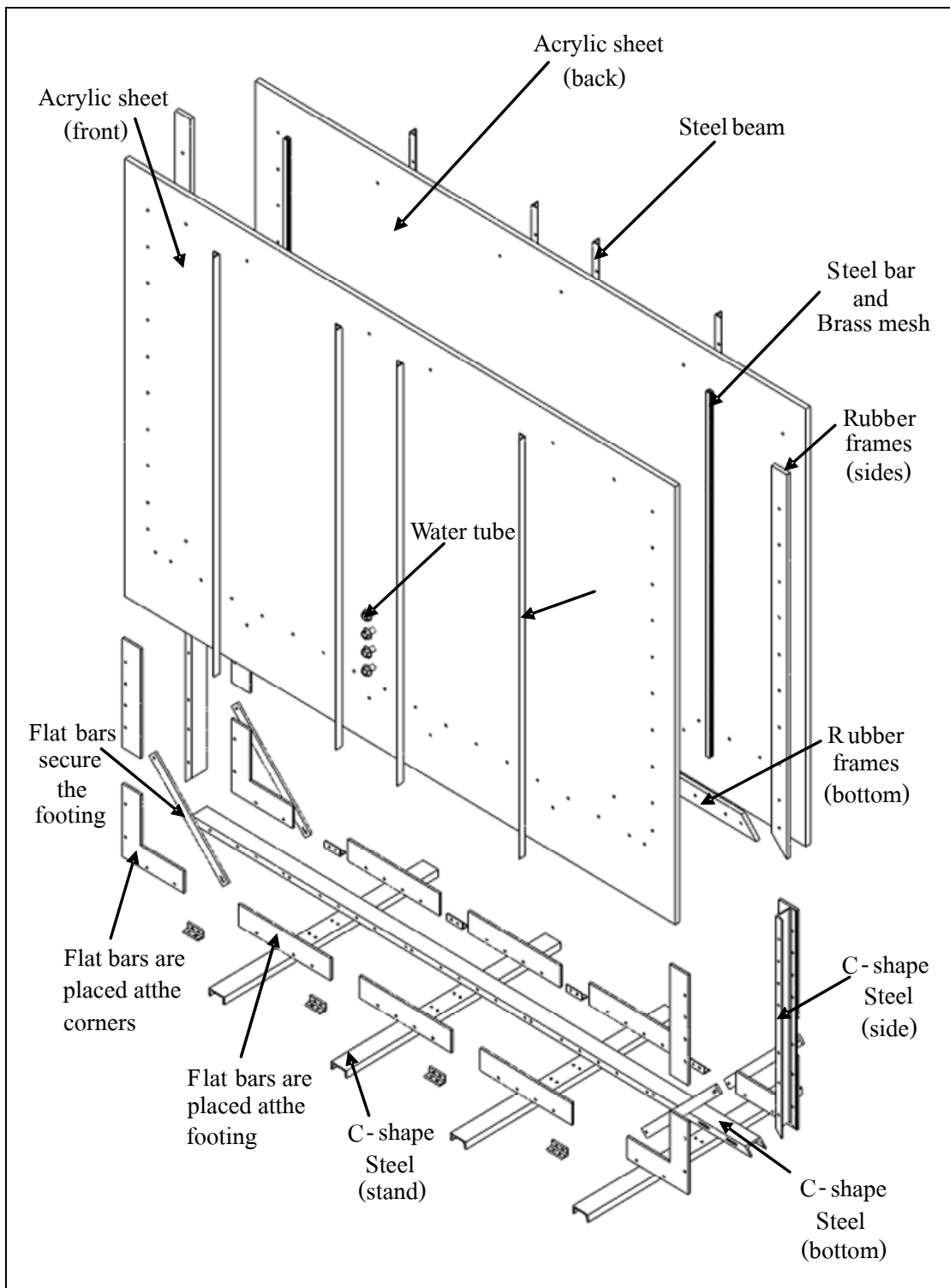


**Figure 3.2** Components of the test frame.

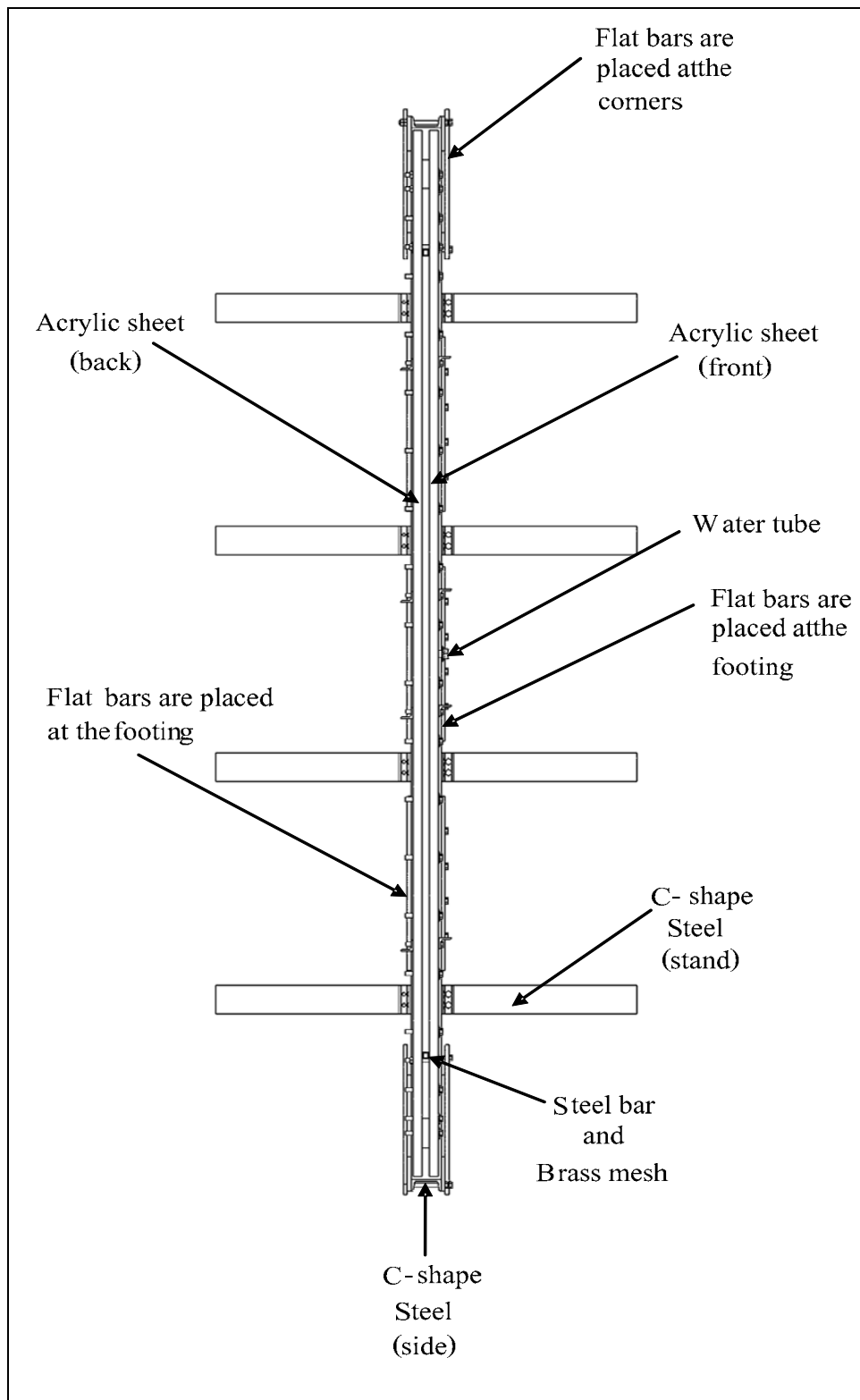


**Figure 3.3** Top view of test frame

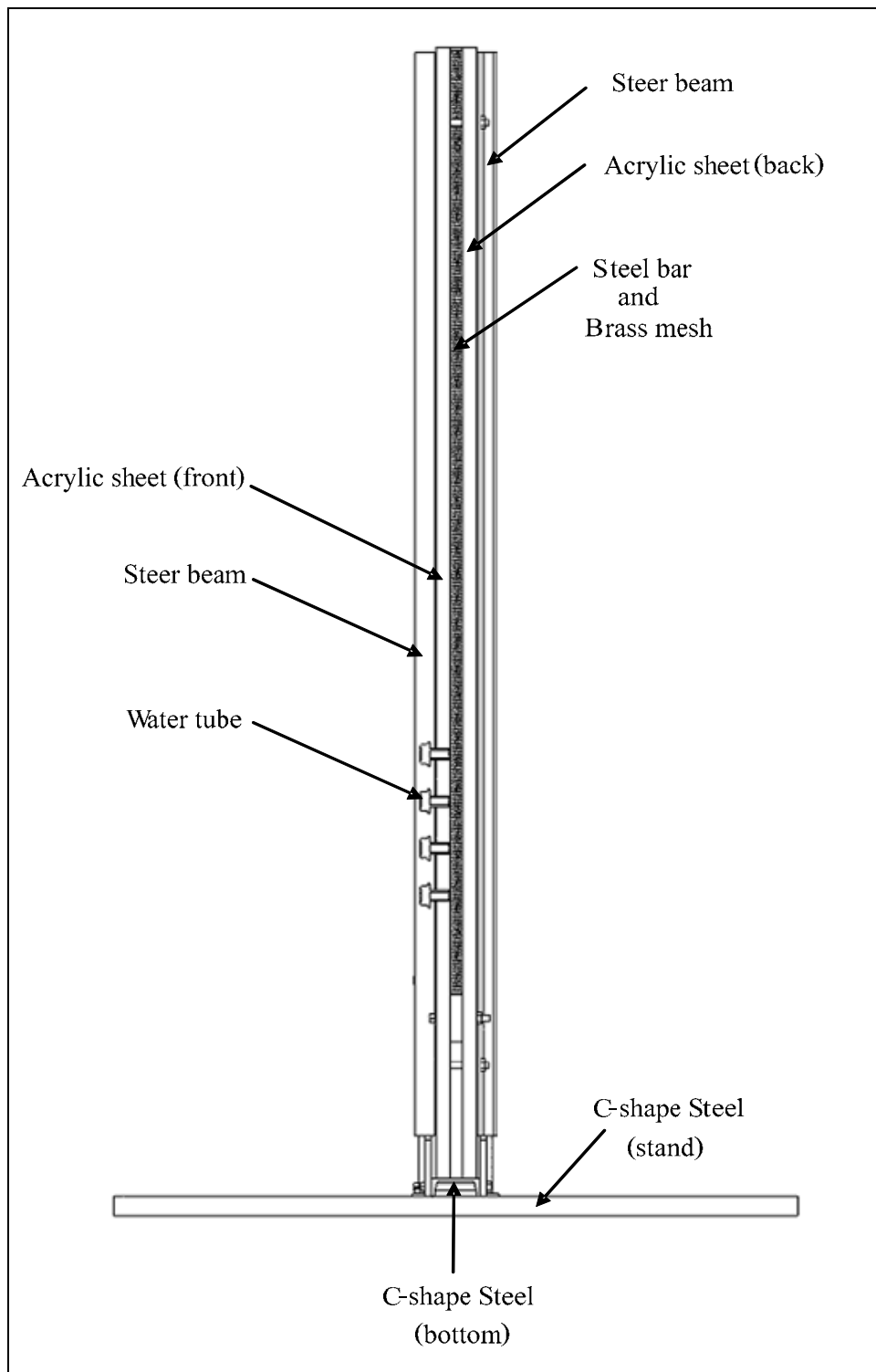


**Figure 3.4** Side view of test frame

Several monitoring points can be accessed in the simulated aquifer by using several pre-designed drill holes on the rear acrylic sheet. These holes have a diameter of 0.5 mm. They are always plugged during the flow testing except when salinity of the water at that location is needed. The test frame and arrangement allow testing the effects of difference in groundwater levels, aquifer thicknesses, distances from the shoreline, and permeability of the shoreline reservoir. Though not included in this research, the test arrangement can simulate the seawater intrusion of the unconfined aquifer(s). Figure 3.5 shows the positions of monitoring points on the rear acrylic plate. The designated  $\Delta h$  is head differences,  $Q$  is flow rate of discharge,  $Q_{FR}$  is flow rate of fresh water pumping,  $Q_{SE}$  is flow rate of salt water extraction,  $Q_{IN}$  is flow rate of fresh water injection and  $D_B$  is depth of subsurface barrier. These monitoring points are used to measure the salinity of the fluid circulating in the model under various test conditions.

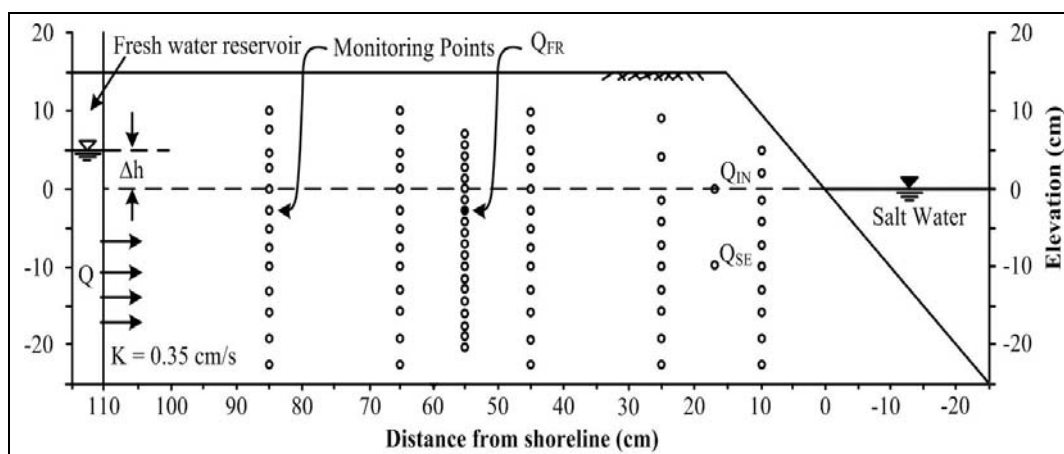


**Figure 3.5** Test parameters and locations of monitoring points on acrylic sheets

# CHAPTER IV

## LABORATORY EXPERIMENTS

### 4.1 Introduction

This chapter describes the method and results of the simulations of seawater intrusion into unconfined aquifers. Series of simulations are carried out to assess the efficiency of the controlling methods by using scaled-down physical models. The controlling methods studied here include extraction of salt water, injection of fresh water and subsurface barrier along the shoreline.

### 4.2 Test Method

This tests are divided into 5 series including natural condition, water pumping condition, extraction of salt water, injection of fresh water and subsurface barrier. Clean sorted sand (0.6-0.8 mm) is used to simulate the unconfined aquifer. The aquifer is 40 cm thick and 140 cm long. The right side of the aquifer is formed 45 degrees inclination slope. Table 4.1 describes the utilized test parameters:  $\Delta h$  is head differences,  $Q$  is the flow rate of discharge,  $Q_{FR}$  is the flow rate of fresh water pumping,  $Q_{SE}$  is the flow rate of salt water extraction,  $Q_{IN}$  is the flow rate of fresh water injection, and  $D_B$  is the depth of subsurface barrier. Figure 4.1 shows the test arrangement. Figure 4.2 shows the positions of monitoring points on the rear acrylic sheet. These points are used to measure the salinity of the fluid circulating in the model under various test conditions. A fresh water reservoir is located on the left side of the frame, while the saturated brine reservoir (prepared to simulate the seawater)



with lower head is located on the right side of the frame. Two head differences,  $\Delta h = 5$  and 10 cm, are used in this study. The head difference is maintained constant during each test by continuous supply of fresh water. The brine is maintained 100% saturated during the test. It is prepared by mixing distilled water with pure sodium chloride. There are several outlet holes drilled on the back of the clear acrylic sheet, and hence allowing withdrawal of the fluid samples at various depths and locations of the aquifer. The changes of the water salinity at various points can therefore be monitored as a function of time. All test series are performed under room (ambient) temperature.

### **4.3 Test Results**

The hydraulic conductivity (K) of the simulating sorted sand aquifer is determined by the Darcy test method as 0.35 cm/s

**Table 4.1** Test parameters

Testing series	Test Parameters					
	$\Delta h$ (cm)	Q (cc/min)	$Q_{FR}$ (cc/min)	$Q_{IN}$ (cc/min)	$Q_{SE}$ (cc/min)	$D_B$ (cm)
Natural condition	10	62				
	5	24				
Water pumping	10	62	0.2			
		85	10			
		120	100			
	5	25	5			
		50	30			
		96	70			
Fresh water Injection	5	80	70	7		
		80		15		
		57		50		
Salt water Extraction	5	75	70		15	
		100			50	
		150			100	
Sub-surface barrier	5	96	70			- 5
						- 10
						- 15

#### 4.3.1 Results under natural condition

Under natural condition (no pumping and extraction wells), the two physical models,  $\Delta h = 10$  cm with  $Q = 62$  cc/min and  $\Delta h = 5$  cm with  $Q = 24$  cc/min, are simulated. At  $\Delta h = 10$  cm, the toe of the fresh-saltwater interface is at 25-45 cm from the shoreline comparable with the results calculated from Ghyben-Herzberg equation (Figures 4.4). For  $\Delta h = 5$  cm, the toe of the fresh-saltwater interface observed from the simulation is at 60-65 cm from the shoreline and agrees with the calculated value from the Ghyben-Herzberg equation (Figure 4.5).

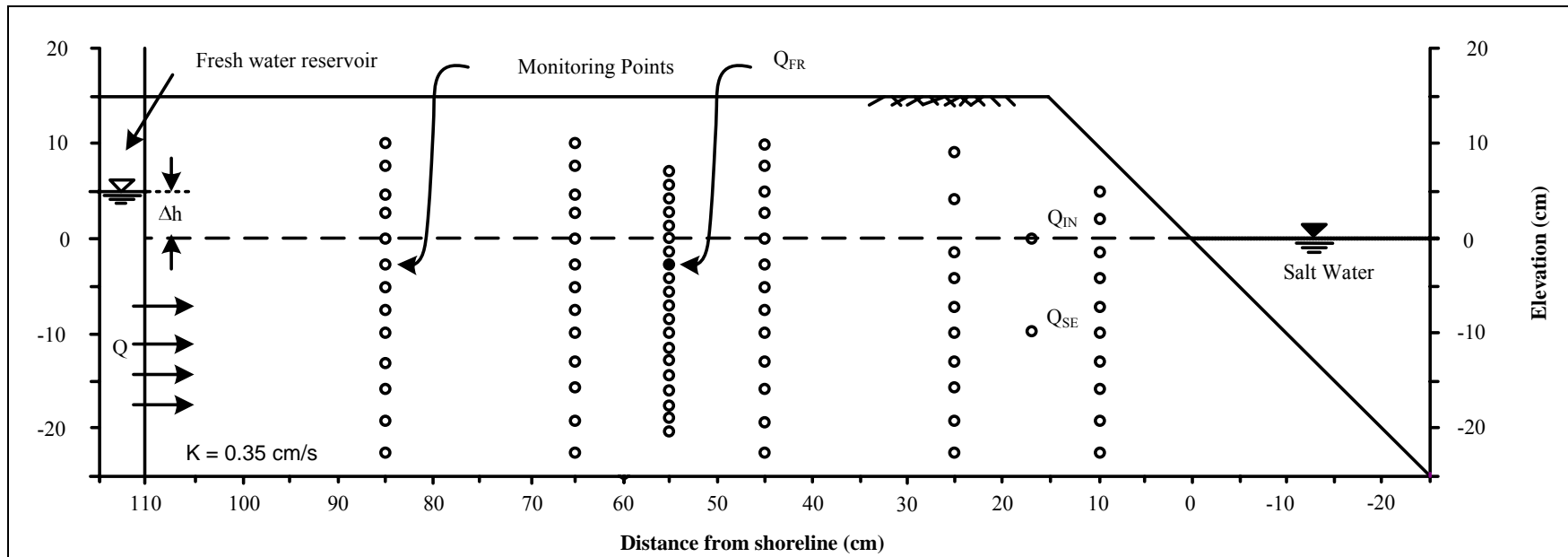


**Figure 4.2** Test parameters and locations of monitoring points on acrylic sheet.

#### 4.3.1.1 Calculate shape of the fresh-salt water interface

Recognizing the approximations inherent in the Ghyben-Herzberg relation, more exact solutions for the shape of the interface have been developed from potential flow theory (Figure 4.3). Has the form (Todd and May, 2005);

$$z^2 = \frac{2\rho qx}{\Delta\rho K} + \left( \frac{\rho q}{\Delta\rho K} \right)^2 \quad (4.1)$$

where  $z$  and  $x$  shown in figure 4.3 ,  $\Delta\rho = \rho_s - \rho_f = 0.23 \text{ g/cm}^3$ ,  $K$  is the hydraulic conductivity of the unconfined aquifer = 0.35 cm/s and  $q$  is the fresh water flow per unit length of shoreline.

The corresponding shape of the water table is given by

$$h_f = \left( \frac{2\Delta\rho qx}{(\rho + \Delta\rho)K} \right)^{1/2} \quad (4.2)$$

The width  $x_0$  of the submarine zone through which fresh water discharges into the sea can be obtained for  $z = 0$ , yielding

$$x_0 = \frac{\rho q}{2\Delta\rho K} \quad (4.3)$$

The depth of the interface beneath the shoreline so that

$$z_0 = \frac{\rho q}{\Delta\rho K} \quad (4.4)$$

From the calculated for  $\Delta h = 10$  cm,  $x_0 = 5.09$  cm and  $\Delta h = 5$  cm,  $x_0 = 1.94$  cm. The result indicated that the fresh-salt water interface observed from the physical model agrees well with the result calculated by the widely known Ghyben-Herzberg equation (Todd and Mays, 2005) for both  $\Delta h = 10$  cm and 5 cm. under natural condition (no pumping and extraction wells). Comparison of the interface profiles obtained from the test and solution for  $\Delta h = 10$  and 5 cm are given in Figures 4.4 and 4.5.

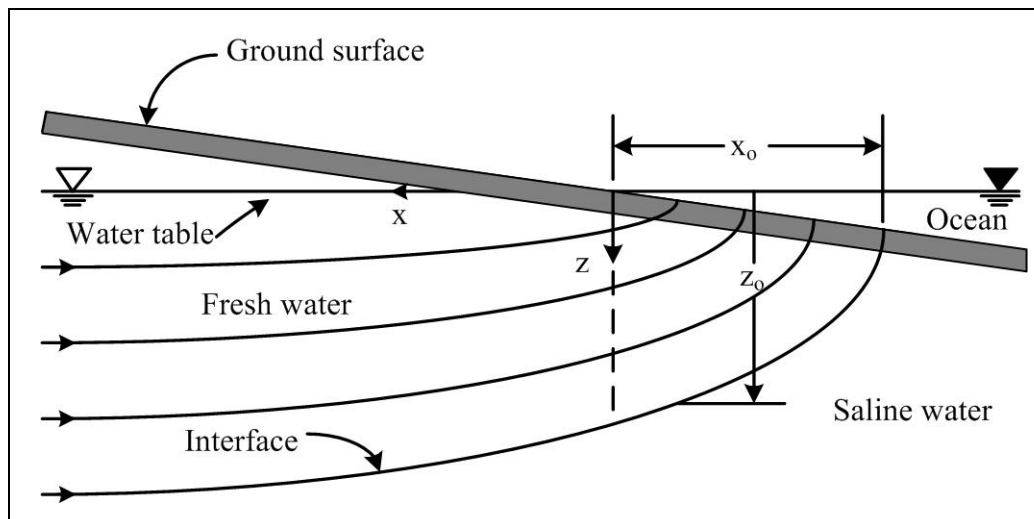


**Figure 4.3** Flow pattern of fresh water in an unconfined coastal aquifer.

### 4.3.2 Simulation of water pumping effect

Six test series for  $\Delta h = 10$  cm with difference  $Q$  are simulated  $\Delta h = 10$  cm with  $Q_{FR} = 0.2, 10$  and  $100$  cc/min (Figures 4.6 through 4.8). The fresh water pumping (usage) is simulated by withdrawing the water at the depth of 2.5 cm below the simulated mean sea level (MSL). The results indicate that the fresh-salt water interface moves toward the pumping location. The lower  $\Delta h$  value shows the shallower interface,

as the interface move toward the pumping well. For  $\Delta h = 5$  cm with  $Q_{FR} = 30$  and 70 cc/min the fresh-saltwater interfaces move 95-110 cm from the shoreline (Figures 4.10 and 4.11). At  $\Delta h = 5$  cm and with the higher the pumping rate, the up-coning characteristics of the interface occur, and eventually the salinity of the pumping well increases (Figures 4.9 through 4.11). The pumping rate is not affected on salinity for higher head difference ( $\Delta h = 10$  cm). The results are given in Table 4.2.

The pumped water however remains fresh as long as the pumping rate ( $Q_{FR}$ ) is less than about 50% of the discharge inflow rate,  $Q$ , (see Table 4.2).

**Table 4.2** Results of water pumping

Testing series	Test Parameters						Results		
	$\Delta h$ (cm)	Q (cc/min)	$Q_{FR}$ (cc/min)	$Q_{SE}$ (cc/min)	$Q_{IN}$ (cc/min)	$D_B$ (cm)	% salinity of pumping well	1 *	2 *
Water pumping	10	62	0.2				0	<-25	<-25
		85	10				0	<-25	-22
		120	100				0	-23	-14
	5	25	5				0	-13	-11
		50	30				20	-10	-9
		96	70				45	-8	-7

Remarks: 1\* Elevations of fresh-salt water interface at pumping location (cm)

2\* Elevations of fresh-salt water interface at half distance between shoreline and pumping location (cm)

#### 4.3.3 Results of the injection of fresh water

Figures 4.12 through 4.14 show the results of the fresh water injection ( $Q_{IN}$ ) with the different rates ( $Q_{IN} = 7, 15$  and 50 cc/min). The injection depth is at the MSL.

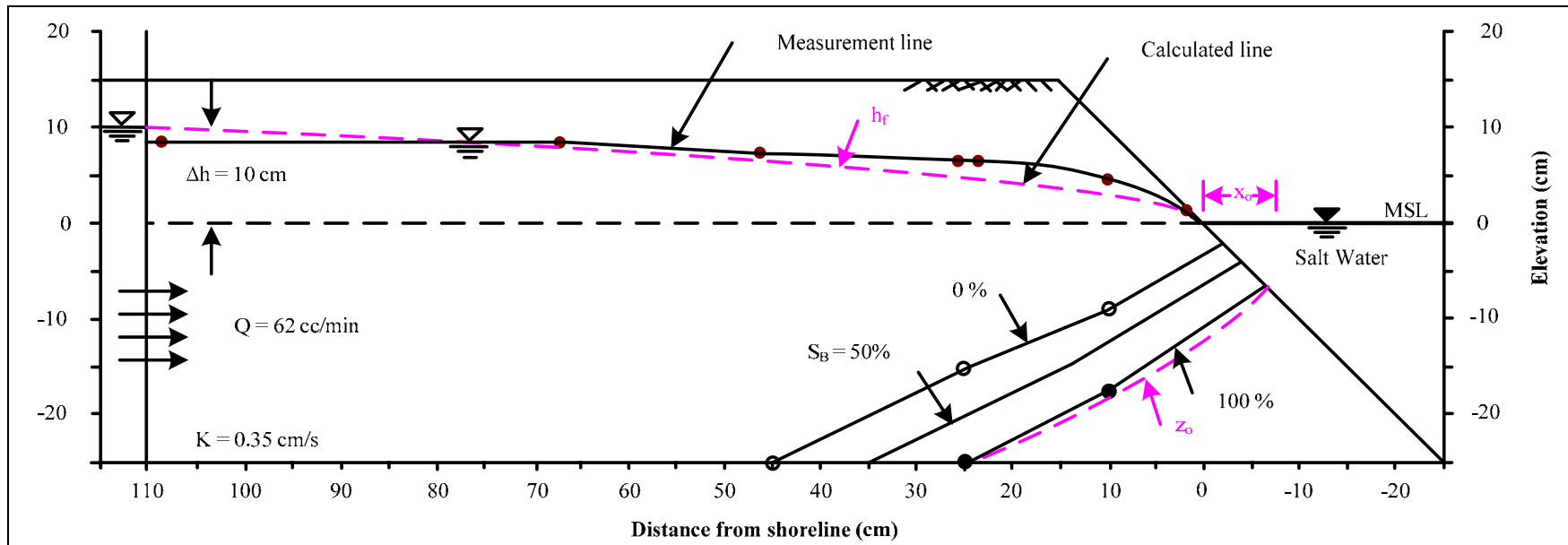


**Figure 4.4** Simulation under natural condition and comparison the results of interface (solid lines) with the Ghyben-Herzberg solution(dash line) at  $\Delta h = 10$  cm

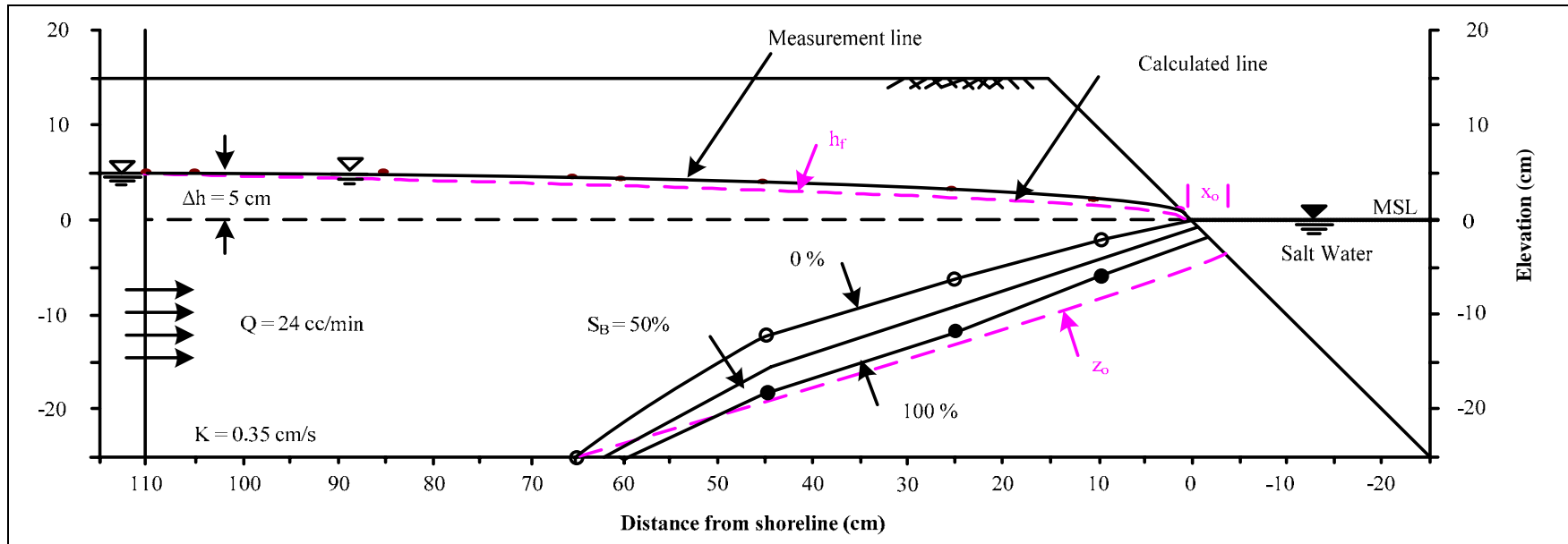


**Figure 4.5** Simulation under natural condition and comparison the results of interface (solid lines) with the Ghyben-Herzberg solution (dash line) at  $\Delta h = 5$  cm

For  $Q_{IN} = 50$  cc/min and  $Q_{FR} = 70$  cc/min condition, as shown in Figures 4.14 the toe of the fresh-saltwater interface is 65 cm from shoreline, and  $Q_{IN} = 15$  cc/min and  $Q_{FR} = 70$  cc/min condition, as shown in Figure 4.13 the toe of the fresh-saltwater interface is 68 cm from shoreline and  $Q_{IN} = 7$  cc/min and  $Q_{FR} = 70$  cc/min condition, as shown in Figure 4.12 the toe of the fresh-saltwater interface is 70 cm from shoreline. The toe of the fresh-saltwater interface decreases with increasing of the freshwater injection rate. The result of the injection of fresh water is zero percentage of salinity of the pumping well. (See Table 4.3)

**Table 4.3** Results of fresh water injection

Testing series	Test Parameters						Results		
	$\Delta h$ (cm)	Q (cc/min)	$Q_{FR}$ (cc/min)	$Q_{SE}$ (cc/min)	$Q_{IN}$ (cc/min)	$D_B$ (cm)	% salinity of pumping well	1 *	2 *
Fresh water Injection	5	80	70		7		0	-18	-10
		80			15			-19	-11
		57			50			-23	-15

Remarks: 1\* Elevations of fresh-salt water interface at pumping location (cm)

2\* Elevations of fresh-salt water interface at half distance between shoreline and pumping location (cm)

#### 4.3.4 Results of the extraction of salt water

The extraction of salt water is simulated by withdrawing the water at the depth of -10 cm and 17 cm distance from shoreline. The salt water pumping rates are 15, 50 and 100 cc/min.

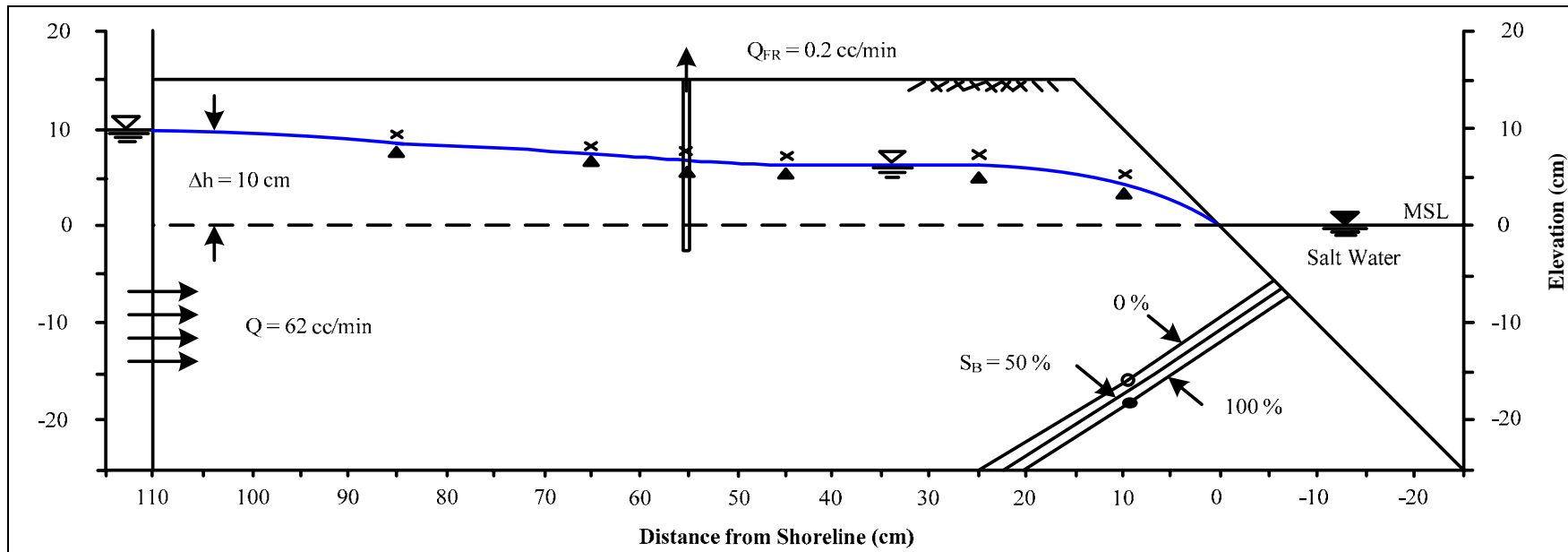


**Figure 4.6** Simulation of water pumping at  $\Delta h = 10 \text{ cm}$ ,  $Q_{FR} = 0.2 \text{ cc/min}$

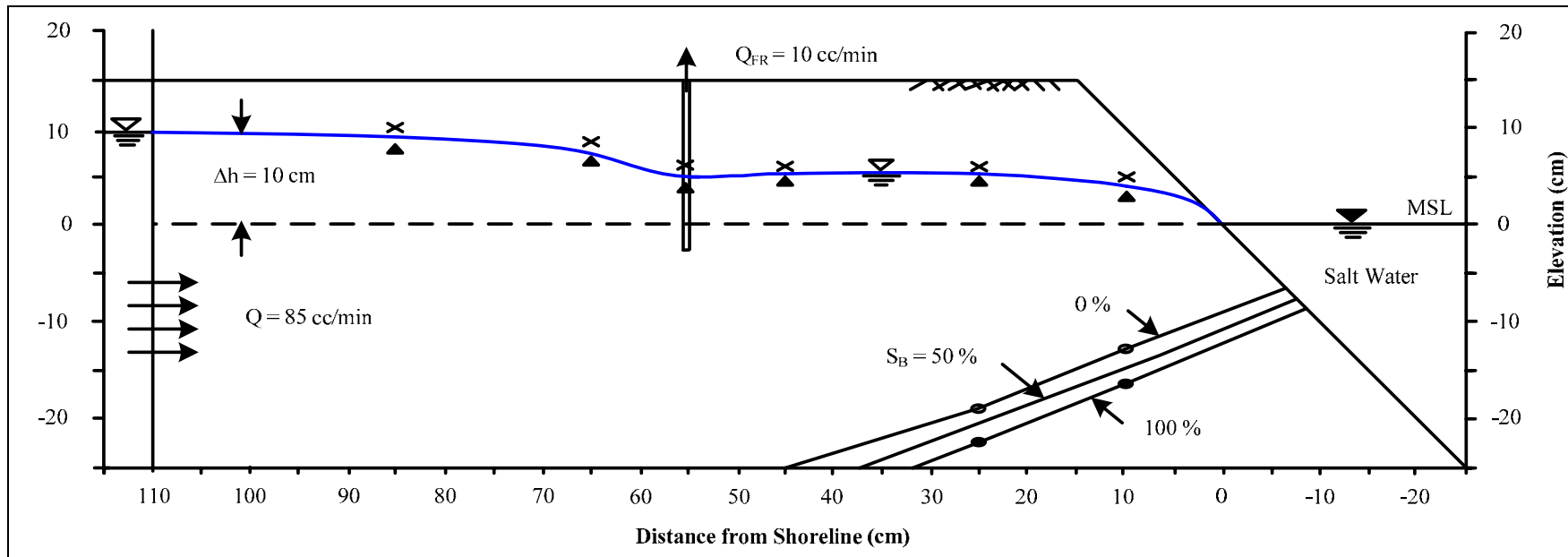


**Figure 4.7** Simulation of water pumping at  $\Delta h = 10 \text{ cm}$ ,  $Q_{FR} = 10 \text{ cc/min}$

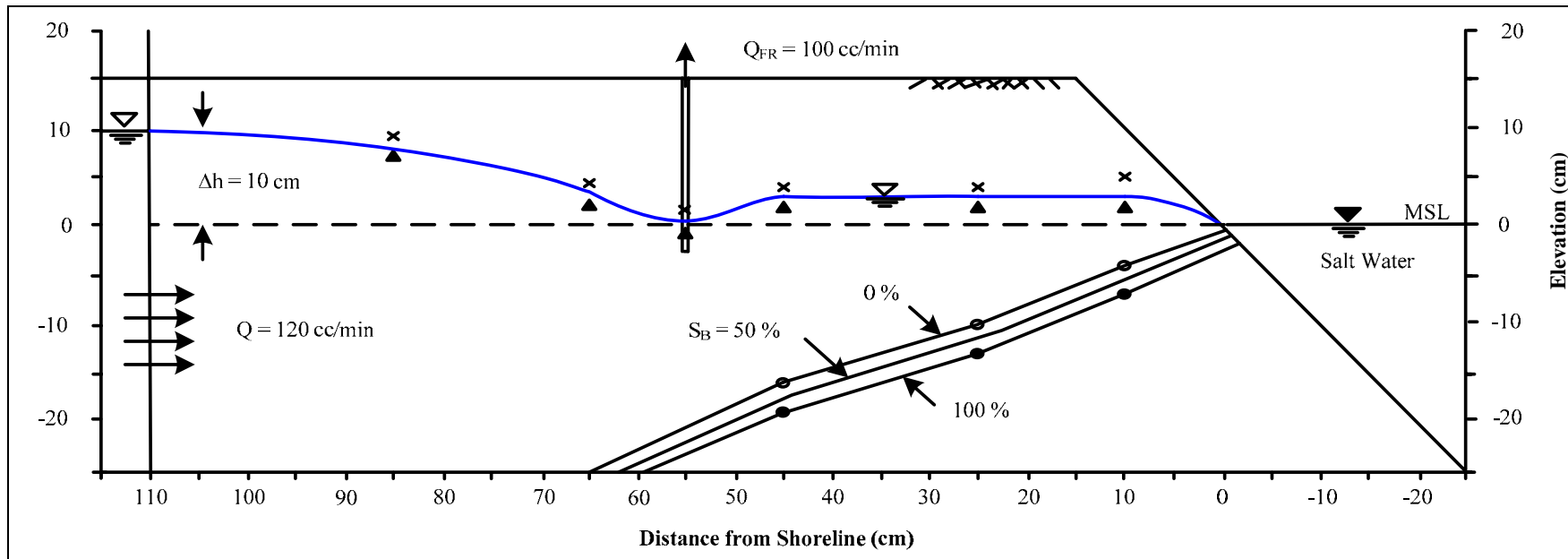


**Figure 4.8** Simulation of water pumping at  $\Delta h = 10 \text{ cm}$ ,  $Q_{FR} = 100 \text{ cc/min}$

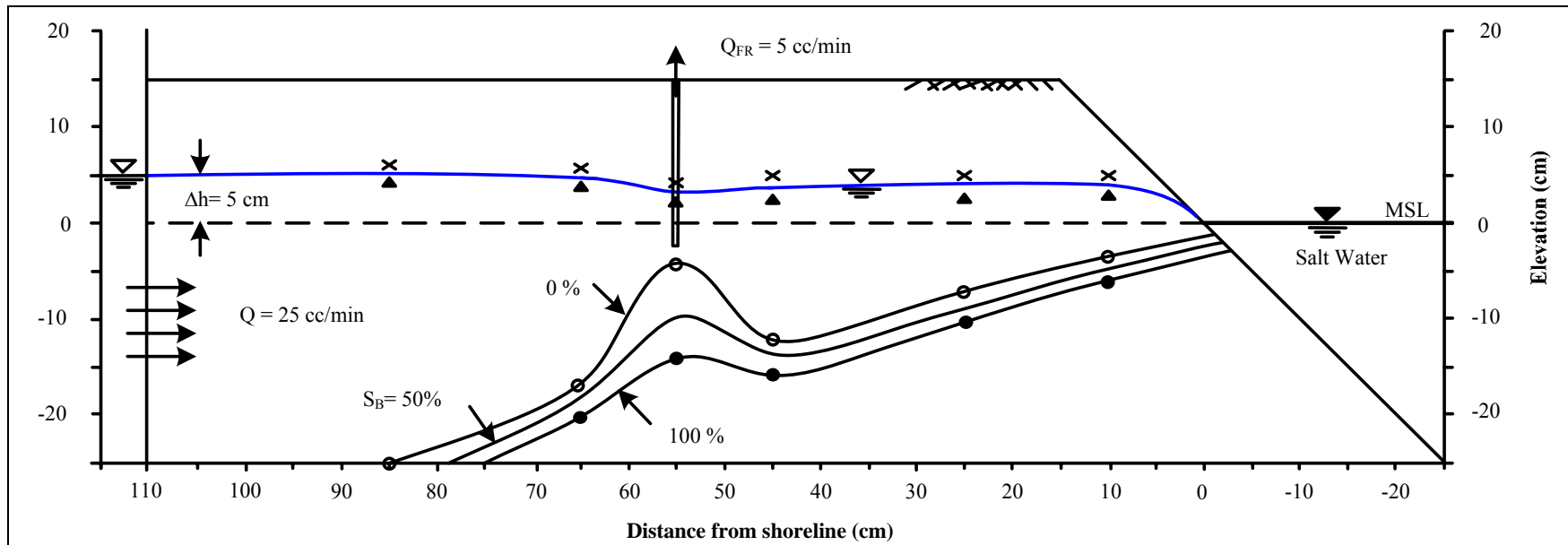


**Figure 4.9** Simulation of water pumping at  $\Delta h = 5 \text{ cm}$ ,  $Q_{FR} = 5 \text{ cc/min}$

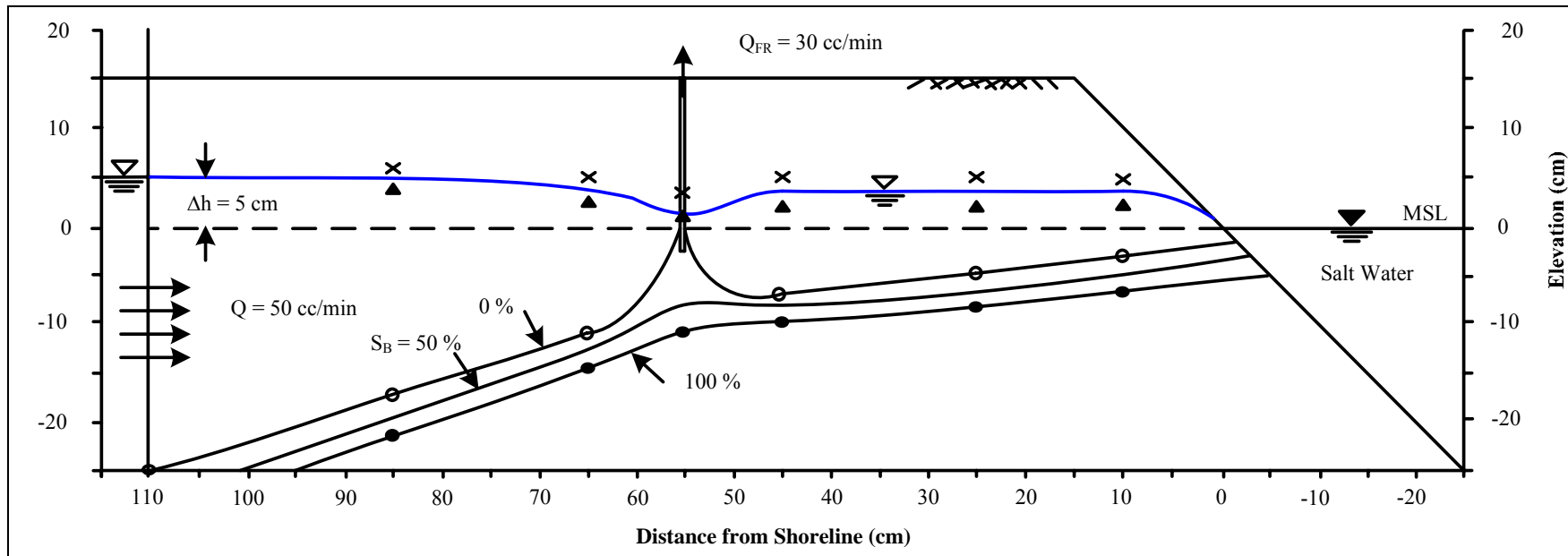


**Figure 4.10** Simulation of water pumping at  $\Delta h = 5 \text{ cm}$ ,  $Q_{FR} = 30 \text{ cc/min}$

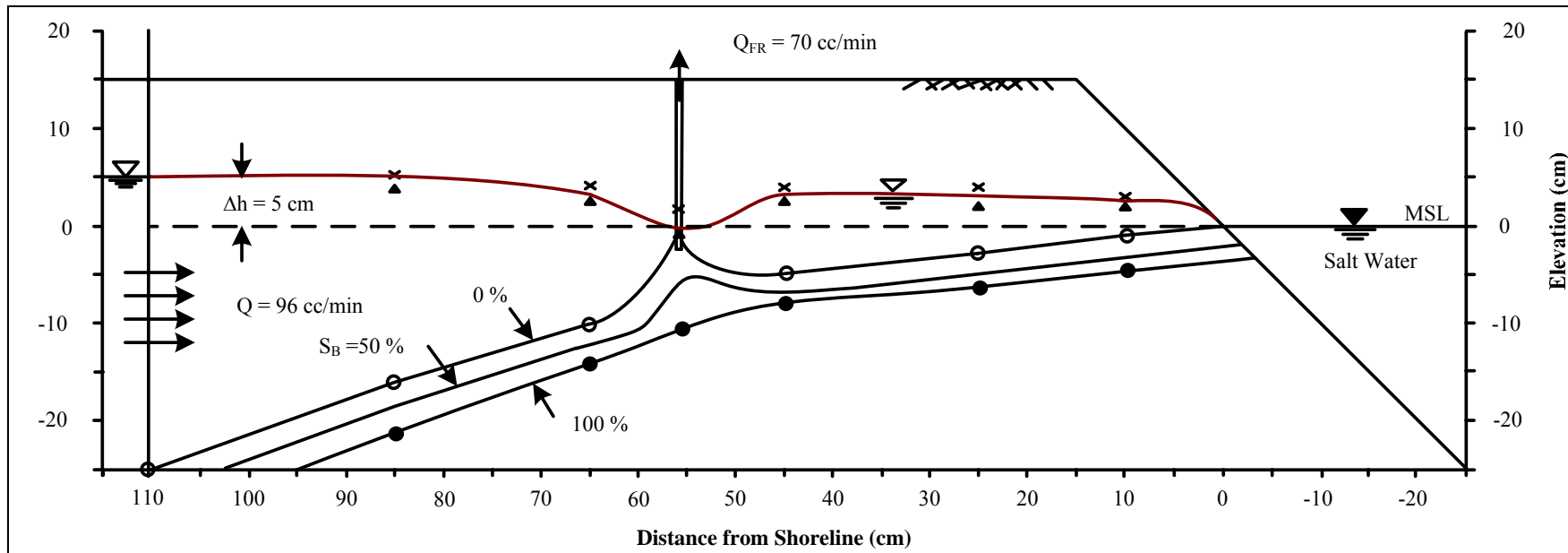


**Figure 4.11** Simulation of water pumping at  $\Delta h = 5$  cm,  $Q_{FR} = 70$  cc/min

For  $Q_{FR} = 70$  cc/min,  $Q_{SE} = 15$  cc/min, the toe of the fresh-saltwater interface is large to 95-110 cm and the salinity of the pumping well is 20 percentage (Figure 4.15). For  $Q_{FR} = 70$  cc/min,  $Q_{SE} = 50$  cc/min the toe of the fresh-saltwater interface is 85-110 cm (Figures 4.16) and for  $Q_{FR} = 70$  cc/min,  $Q_{SE} = 100$  cc/min the toe of the fresh-saltwater interface is 65-85 cm (Figure 4.17), the salinity of the pumping well is fresh well. The results indicate that salt water extraction is effective only when the extraction rate ( $Q_{SE}$ ) is greater than the water usage ( $Q_{FR}$ ) (See Table 4.4).

**Table 4.4** Results of salt water extraction

Testing series	Test Parameters						Results		
	$\Delta h$ (cm)	Q (cc/min)	$Q_{FR}$ (cc/min)	$Q_{SE}$ (cc/min)	$Q_{IN}$ (cc/min)	$D_B$ (cm)	% salinity of pumping well	1 *	2 *
Salt water Extraction	5	75	70	15			20	-8	-5
		100		50			0	-15	-10
		150		100			0	-22	-13

Remarks: 1\* Elevations of fresh-salt water interface at pumping location (cm)

2\* Elevations of fresh-salt water interface at half distance between shoreline and pumping location (cm)

#### 4.3.5 Result of the subsurface barrier

The subsurface barrier is simulated by creating a vertical zone near the shoreline with a permeability about half of the sand aquifer. The results suggest that there is an optimum barrier depth that can reduce the salinity of the water usage well. The shallow barrier (-5 cm below MSL), the toe of the fresh-saltwater interface is 68-85 cm from the shoreline and pumping used is zero percentage, can keep the pumping water well fresh by reducing the flow of the sea into the

unconfined aquifer (Figure 4.18). The deep barrier (-15 cm below MSL), the toe of the fresh-saltwater interface is 95-110 cm from the shoreline, can also keep the water well fresh by minimizing the intrusion of the sea water at the depth above the impermeable layer (Figures 4.20). However for the intermediate barrier at the depth of -10 cm below MSL, it can not keep the pumping water well fresh and the toe of the fresh-saltwater interface is 95-110 cm from the shoreline (Figure 4.19) and See Table 4.5

**Table 4.5** Results of subsurface barrier

Testing series	Test Parameters						Results		
	$\Delta h$ (cm)	Q (cc/min)	$Q_{FR}$ (cc/min)	$Q_{SE}$ (cc/min)	$Q_{IN}$ (cc/min)	$D_B$ (cm)	% salinity of pumping well	1 *	2 *
Sub- surface barrier	5	96	70			- 5	0	-17	-9
						- 10	15	-11	-7
						- 15	0	-15	-8

Remarks: 1\* Elevations of fresh-salt water interface at pumping location (cm)

2\* Elevations of fresh-salt water interface at half distance between shoreline and pumping location (cm)

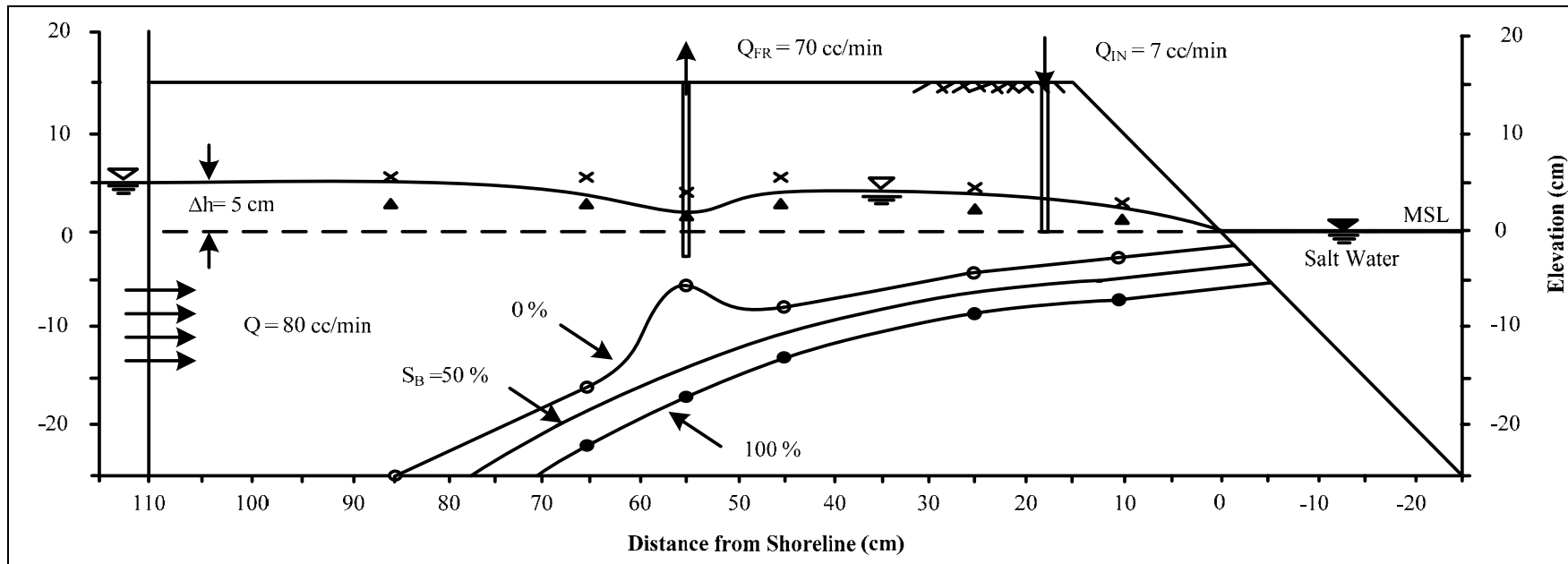


**Figure 4.12** Simulation of fresh water injection at MSL,  $Q_{IN} = 7 \text{ cc/min}$

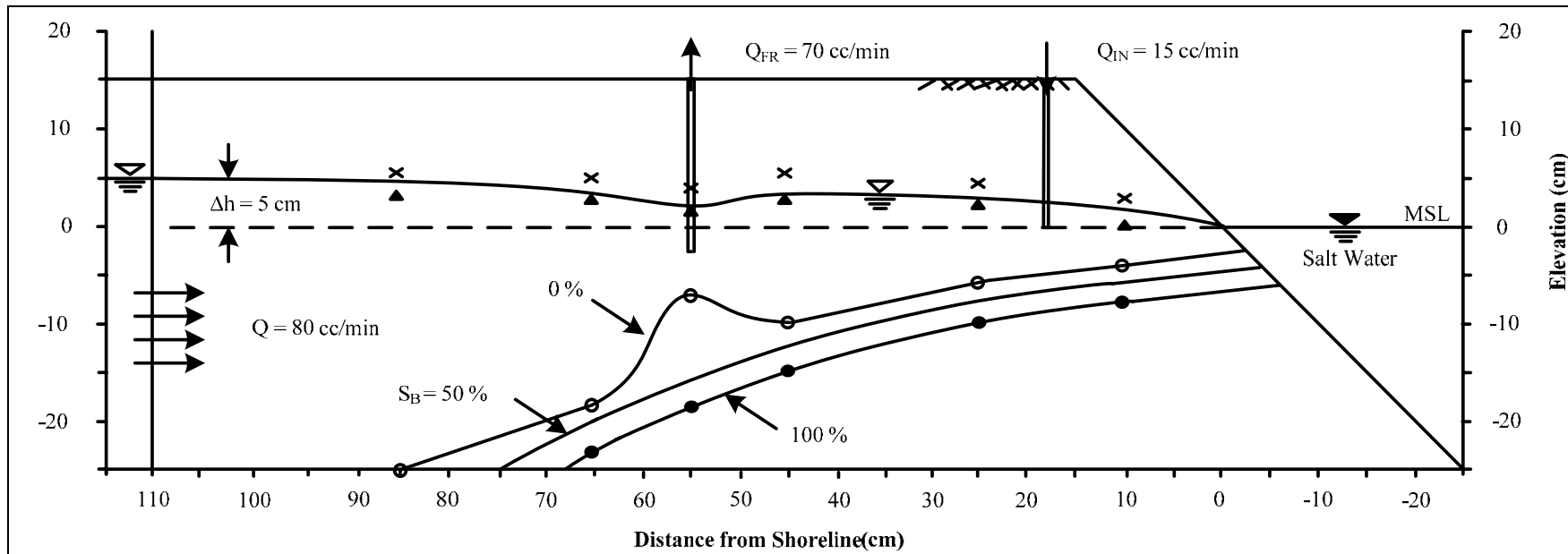


**Figure 4.13** Simulation of fresh water injection at MSL,  $Q_{IN} = 15 \text{ cc/min}$

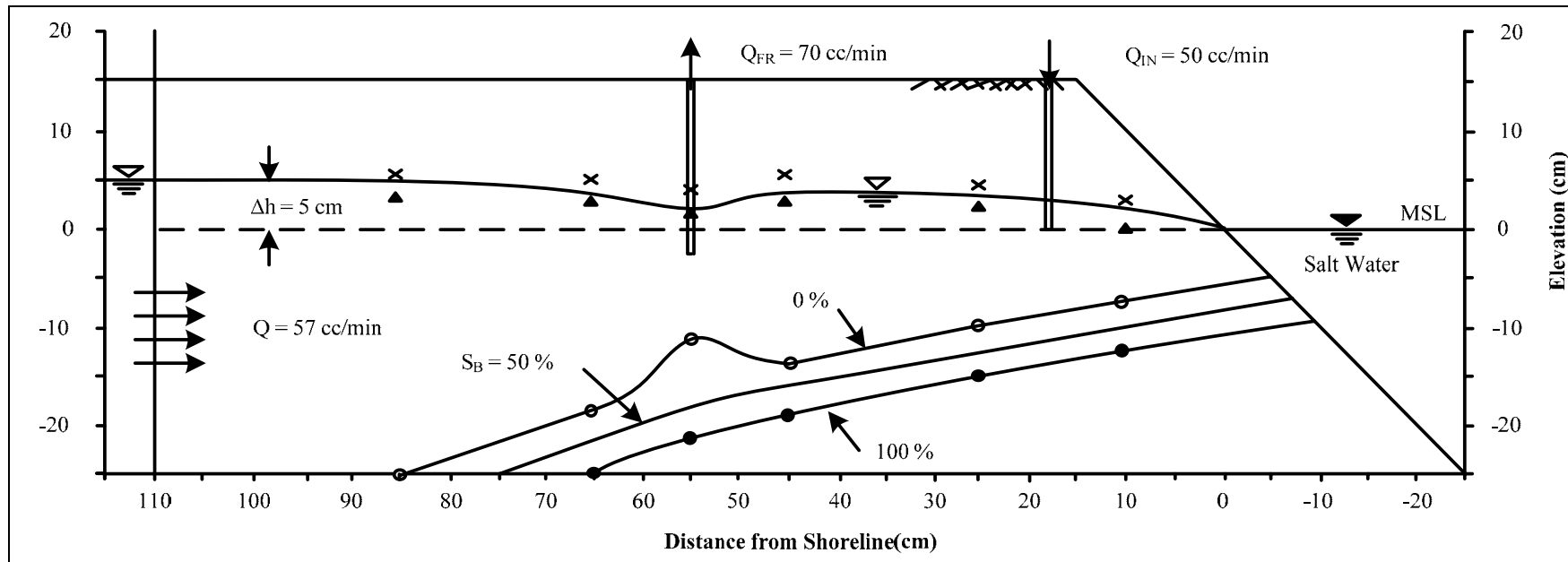


**Figure 4.14** Simulation of fresh water injection at MSL,  $Q_{IN} = 50$  cc/min

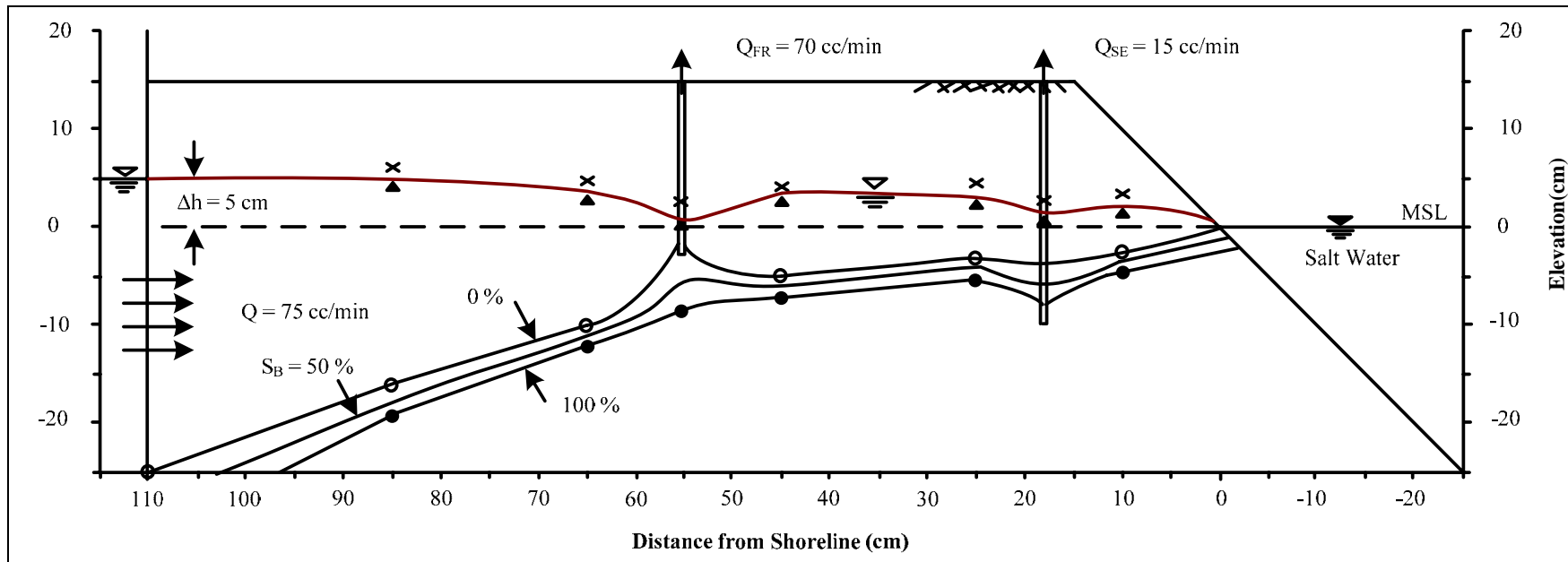


**Figure 4.15** Simulation of salt water extraction at  $-10$  cm,  $Q_{SE} = 15$  cc/min

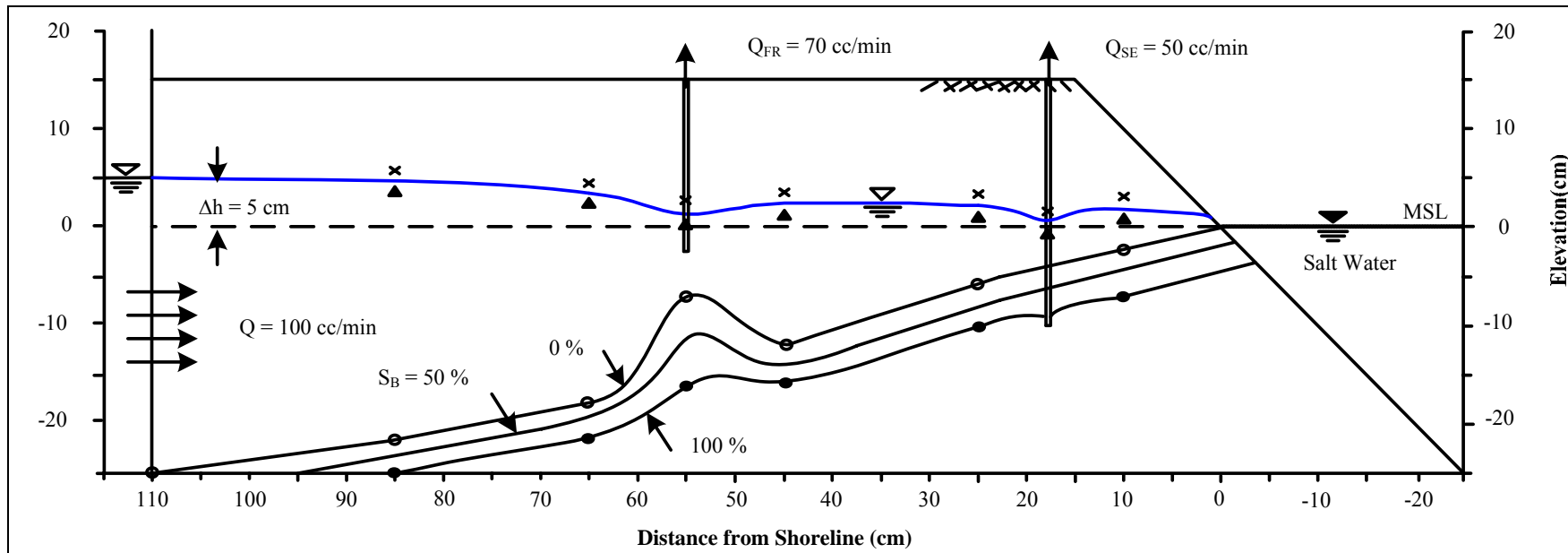


**Figure 4.16** Simulation of salt water extraction at  $-10 \text{ cm}$ ,  $Q_{SE} = 50 \text{ cc/min}$

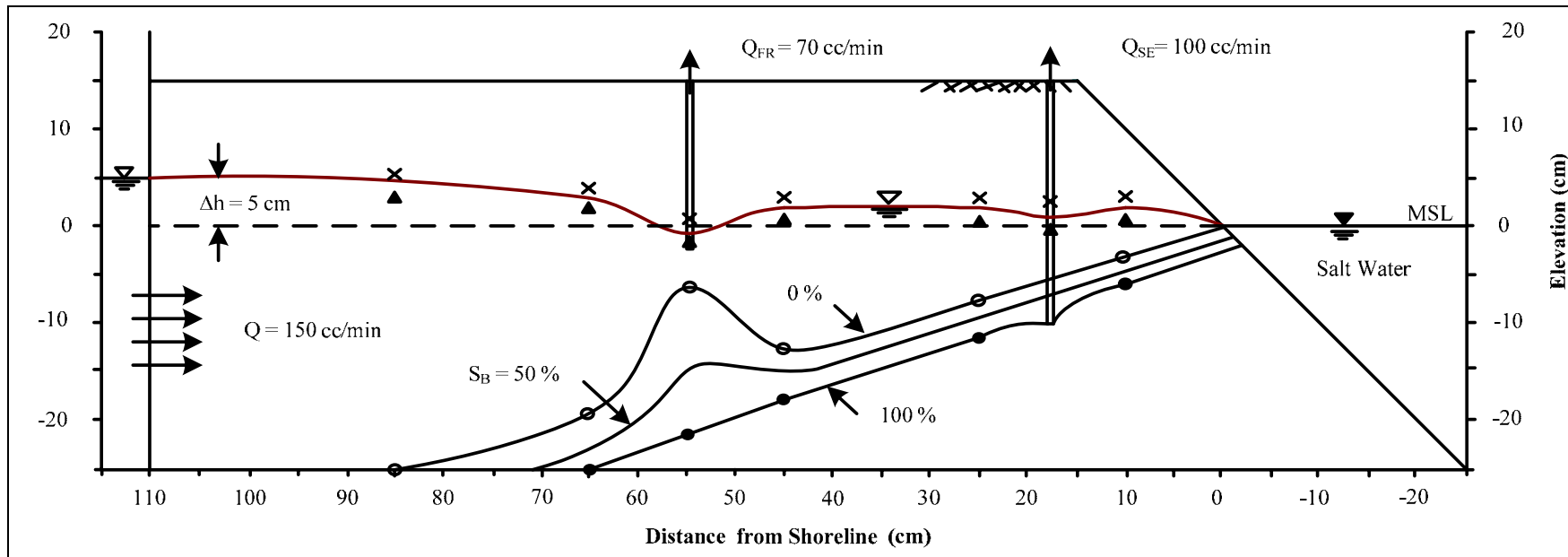


**Figure 4.17** Simulation of salt water extraction at  $-10$  cm,  $Q_{SE} = 100$  cc/min

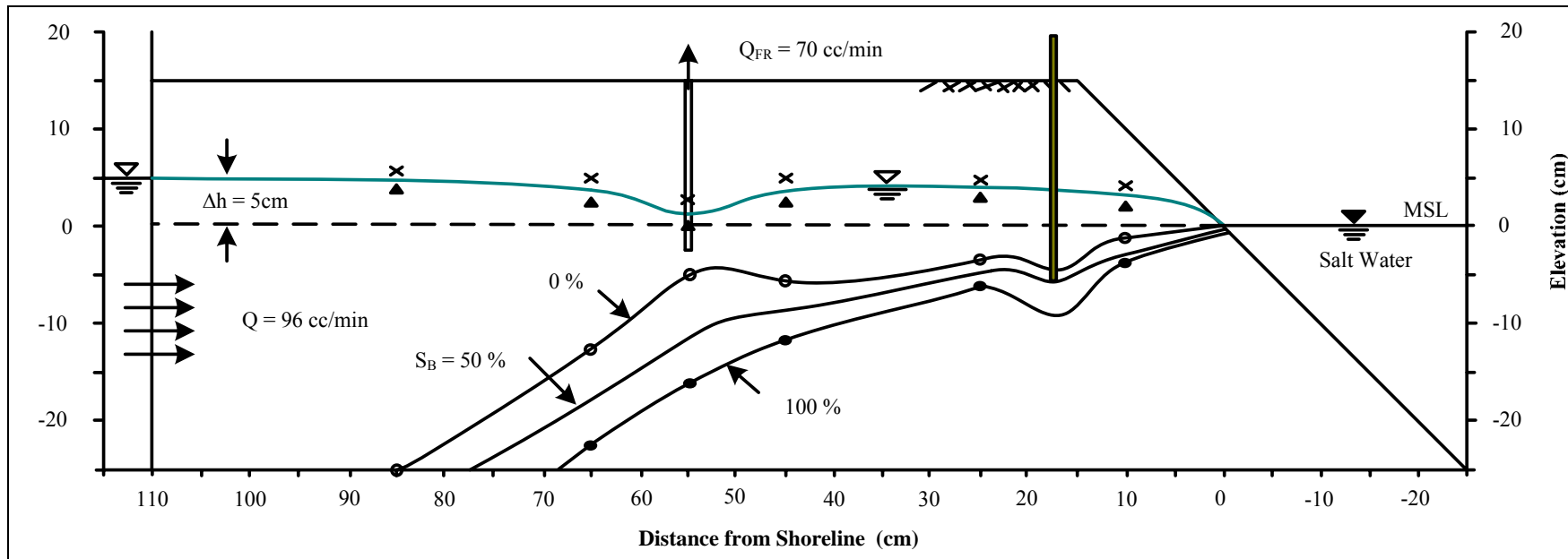


**Figure 4.18** Simulation of at subsurface barrier at  $D_B = -5$  cm

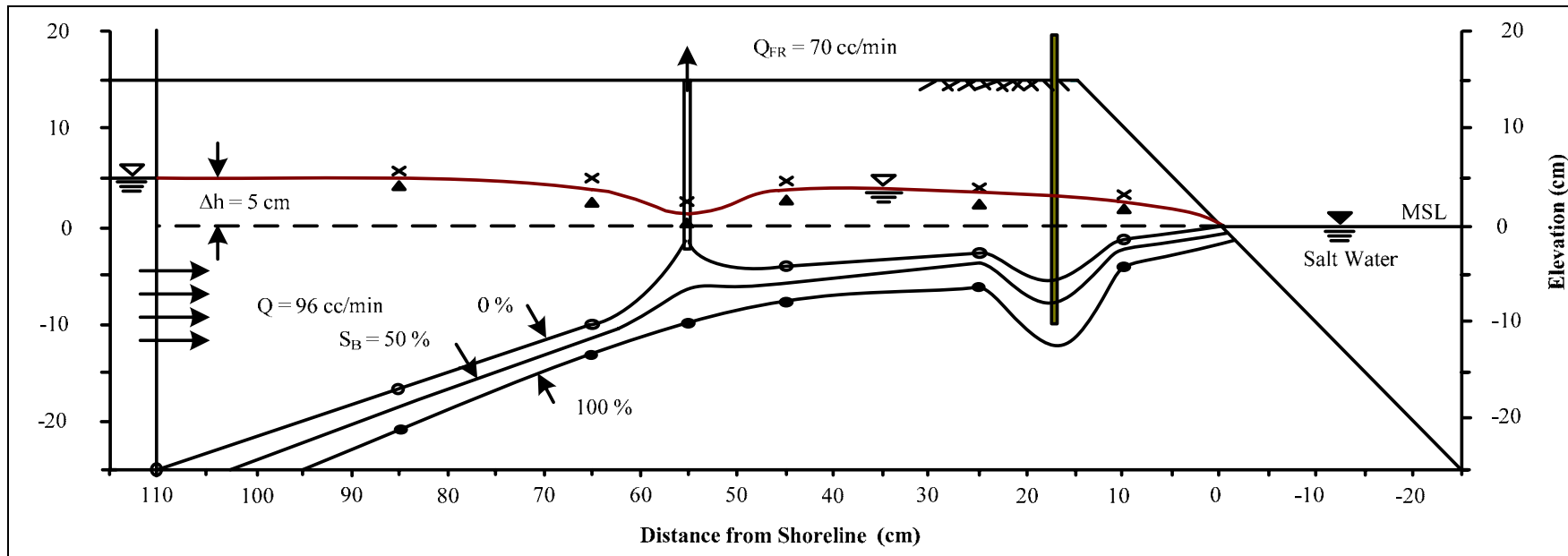


**Figure 4.19** Simulation of at subsurface barrier at  $D_B = -10$  cm

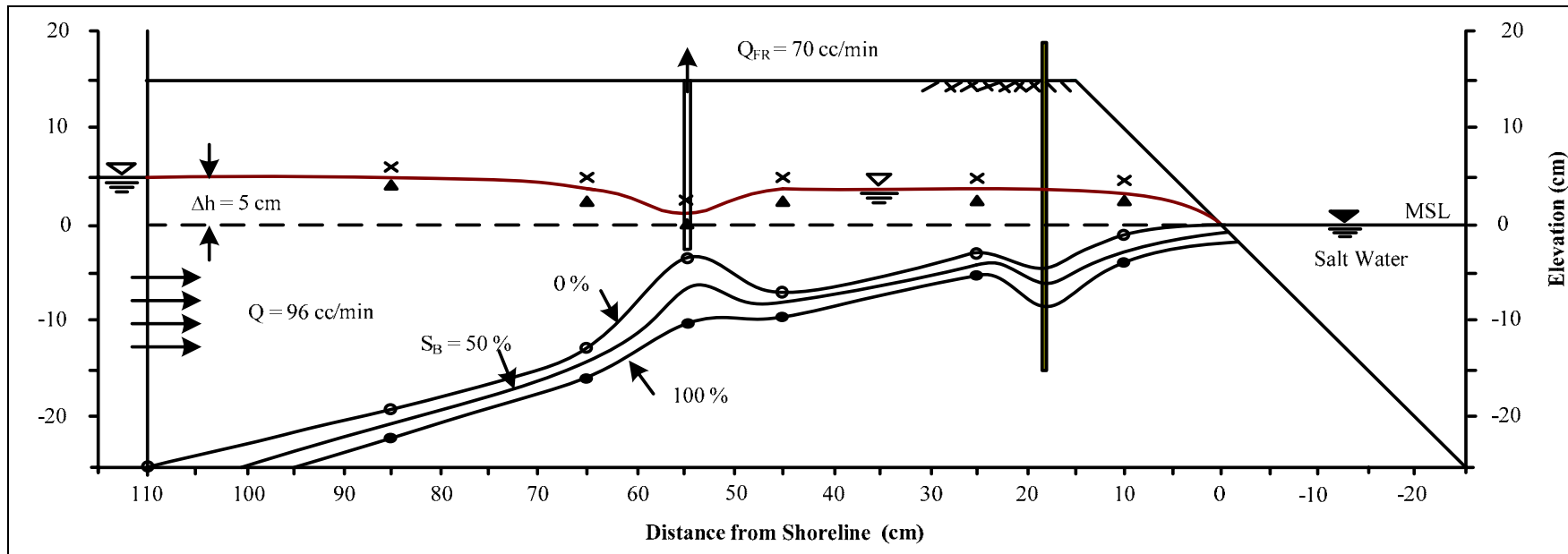


**Figure 4.20** Simulation of at subsurface barrier at  $D_B = -15$  cm

# **CHAPTER V**

## **DYE TESTING**

### **5.1 Objective**

The objective of dye testing into allows a visual inspection of the salt-fresh water interface that moves toward the pumping well. The tests are performed under five conditions: natural condition, water pumping condition, injection of fresh water, extraction of salt water and subsurface barrier.

### **5.2 Test methods**

In this test, red dye is dissolved in the salt water for observing the migration to the unconfined aquifer. Since only small amount of the dye in used (5-10cc), the property of the salt water in unchanged. The test for each series in then started after the mixture content is consistent.

### **5.3 Results for natural condition**

For the natural condition the dye testing in performed under the following parameters:  $\Delta h = 10$ ,  $Q = 62$  cc/min and  $\Delta h = 5$  cm,  $Q = 24$  cc/min Figures 5.1 and 5.2 shows the results for both cases. The interface between the saltwater and fresh water can be clearly seen. The saltwater intrusion for the lower  $\Delta h$  is clearly greater than that for the higher  $\Delta h$  value. This agrees very well with those obtained previously in Chapter IV.

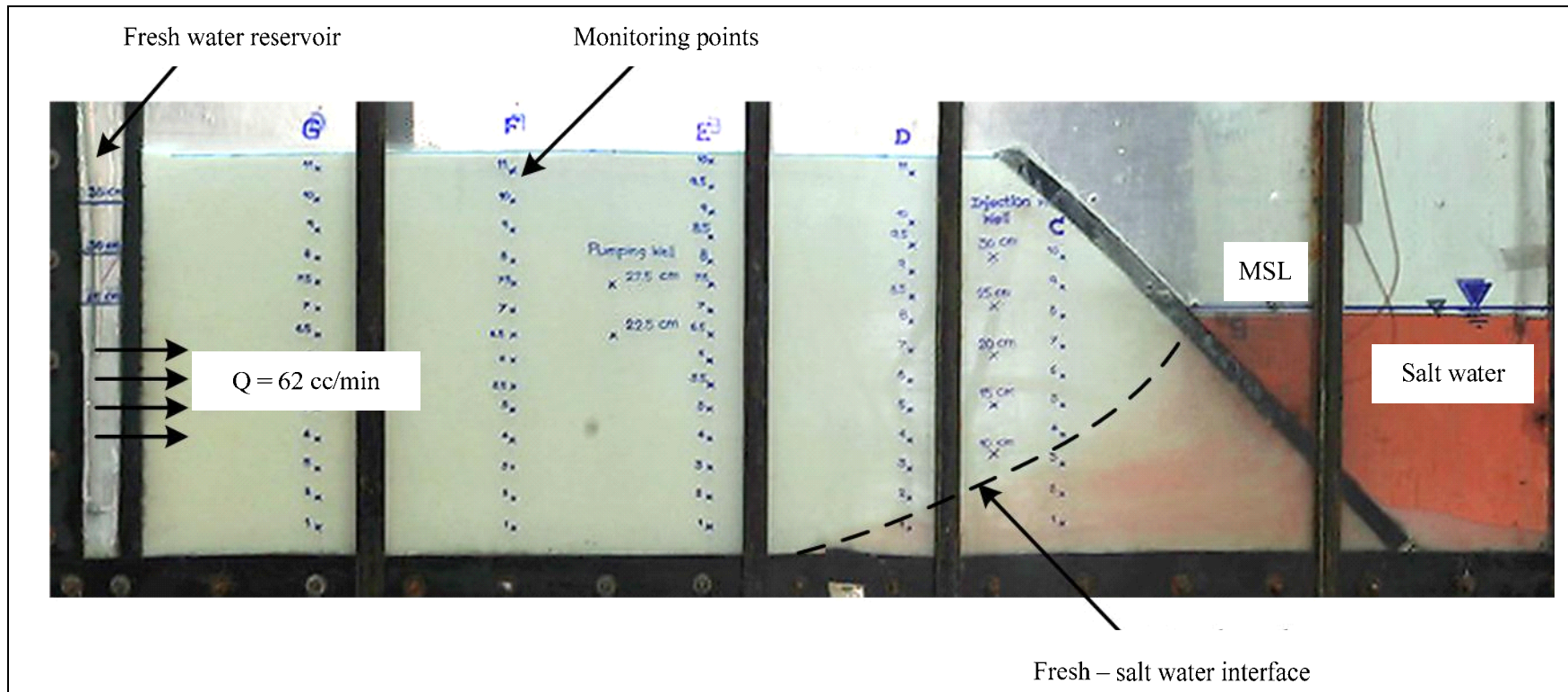


**Figure 5.1** Dye testing under natural condition at  $\Delta h = 10$  cm

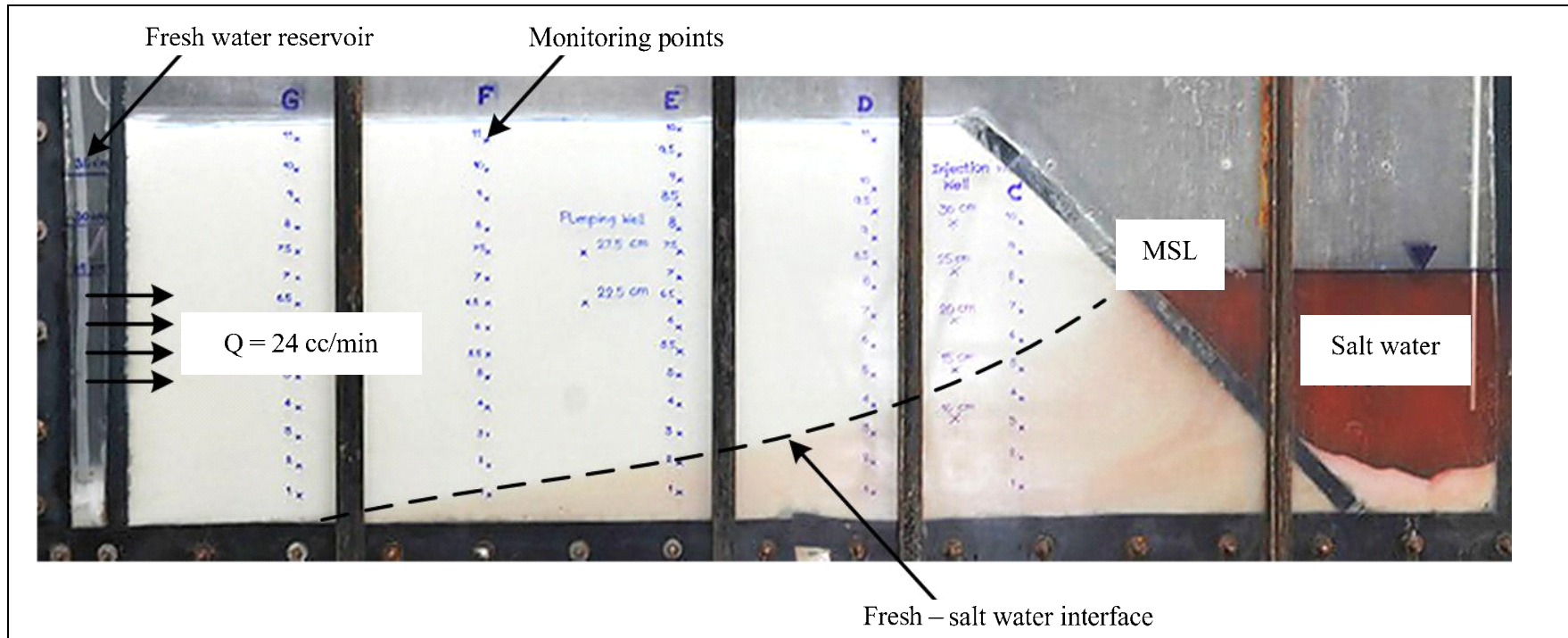


**Figure 5.2** Dye testing under natural condition at  $\Delta h = 5 \text{ cm}$

#### **5.4 Results for water pumping**

For the water pumping condition the dye testing is performed under the following parameters:  $\Delta h = 5$  cm,  $Q_{FR} = 70$ cc/min. The interface between the saltwater and fresh water can be clearly seen. The fresh-salt water interface move 95-110 cm and occurs the up-coning characteristics of the interface and eventually the salinity of the pumping well increases. This agrees very well with those obtained previously in Chapter IV (Figure 5.3).

#### **5.5 Results for injection of fresh water**

For the injection of fresh water condition the dye testing is performed under the following parameters: injection of fresh water at  $\Delta h = 5$  cm,  $Q_{FR} = 70$ cc/min,  $Q_{IN} = 50$  cc/min and location of injection well is mean sea level. The interface between the saltwater and fresh water can be clearly seen. The toe of the fresh-saltwater interface decreases and the pumping well shows zero percentage of salinity. This agrees very well with those obtained previously in Chapter IV (figure 5.4).

#### **5.6 Results for extraction of salt water**

For the extraction of salt water condition the dye testing is performed under the following parameters:  $\Delta h = 5$  cm,  $Q_{FR} = 70$ cc/min and the salt water pumping rate ( $Q_{SE}$ ) = 50 cc/min and location of extraction well is 10 below the mean sea level. The interface between the saltwater and fresh water can be clearly seen (Figure 5.5). The toe of the fresh-saltwater interface is 110 cm. The fresh-salt water interface decrease and the pumping well is fresh. This agrees very well with those obtained previously in Chapter IV.

## **5.7 Results for subsurface barrier**

For the subsurface barrier condition the dye testing is performed under the intermediate subsurface barrier at the depth of 10 cm below mean sea level. The interface between the saltwater and fresh water can be clearly seen. It can not keep the pumping water well fresh and the toe of the fresh-saltwater interface is 100 cm and occurs the up-coning characteristics of the interface as shown in Figure 5.6. This does not agree with those obtained previously in Chapter IV.

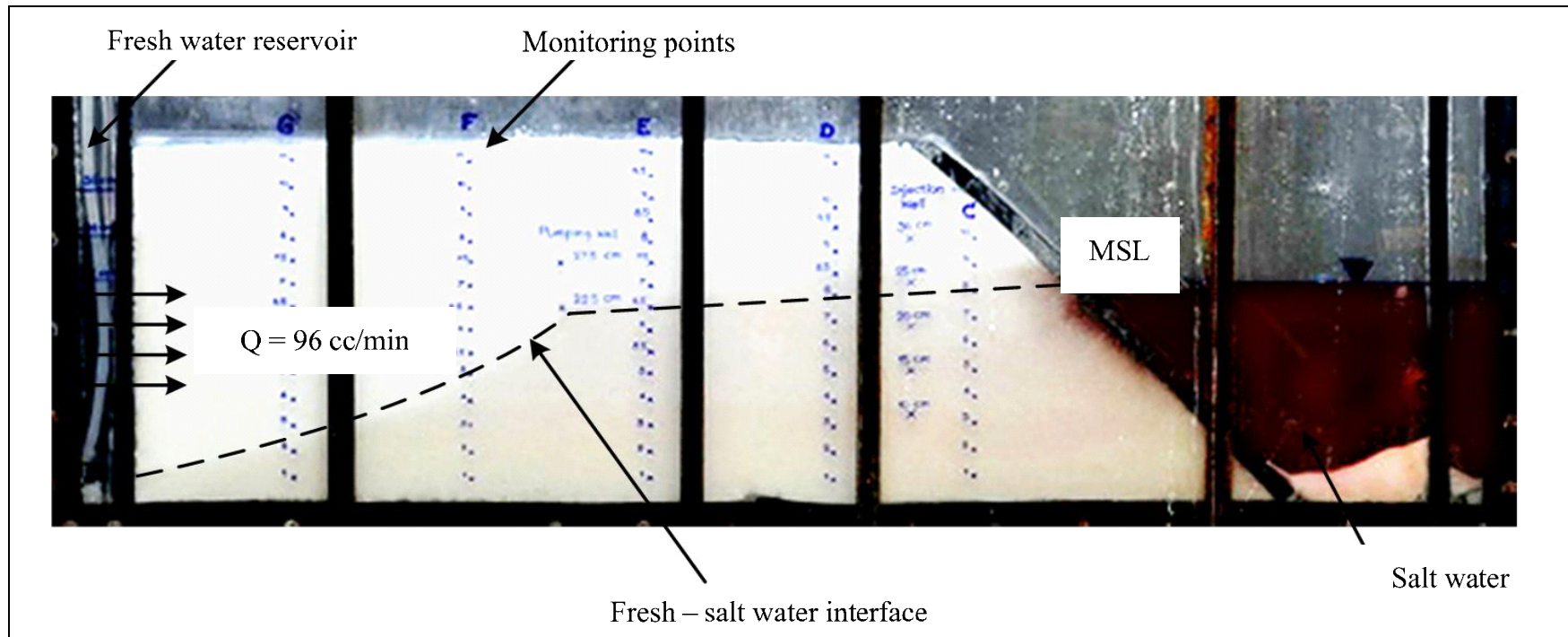


**Figure 5.3** Dye testing for water pumping with  $\Delta h = 5$  cm with  $Q_{FR} = 70$  cc/min

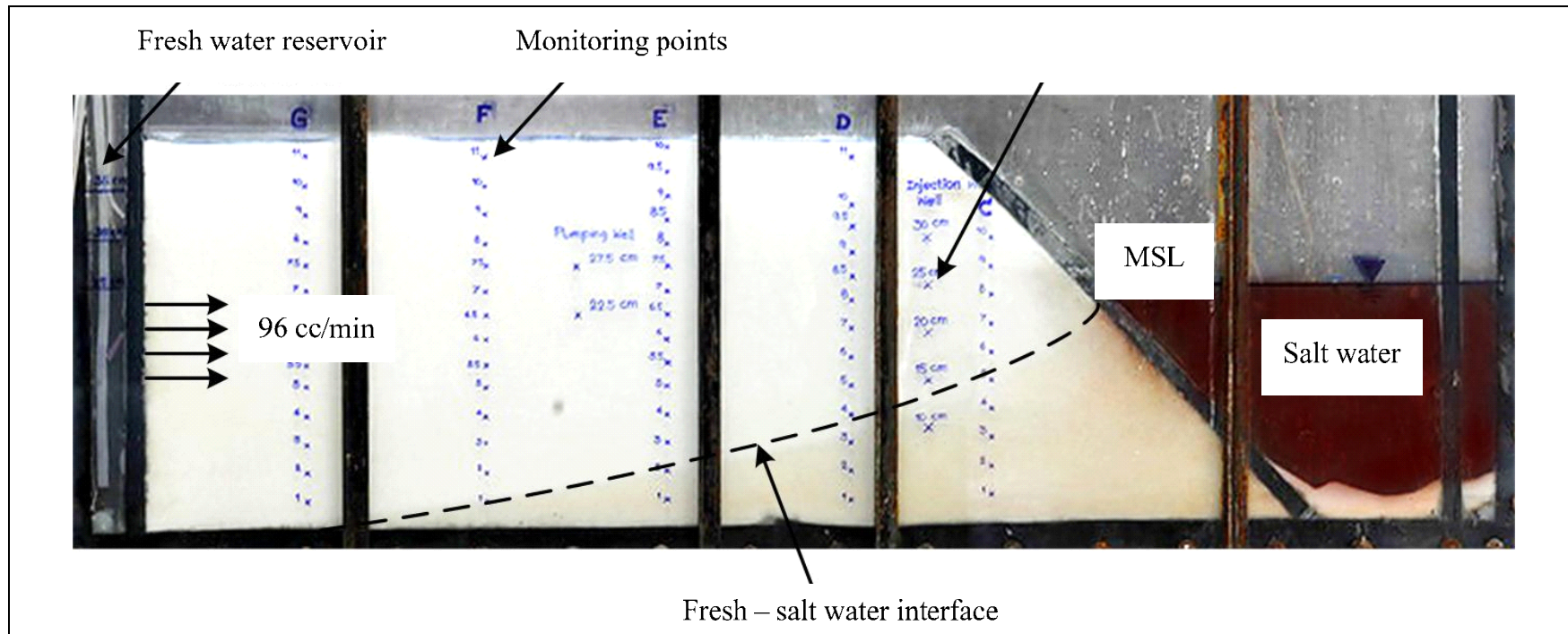


**Figure 5.4** Dye testing for fresh water injection at MSL with  $Q_{IN} = 50$  cc/min

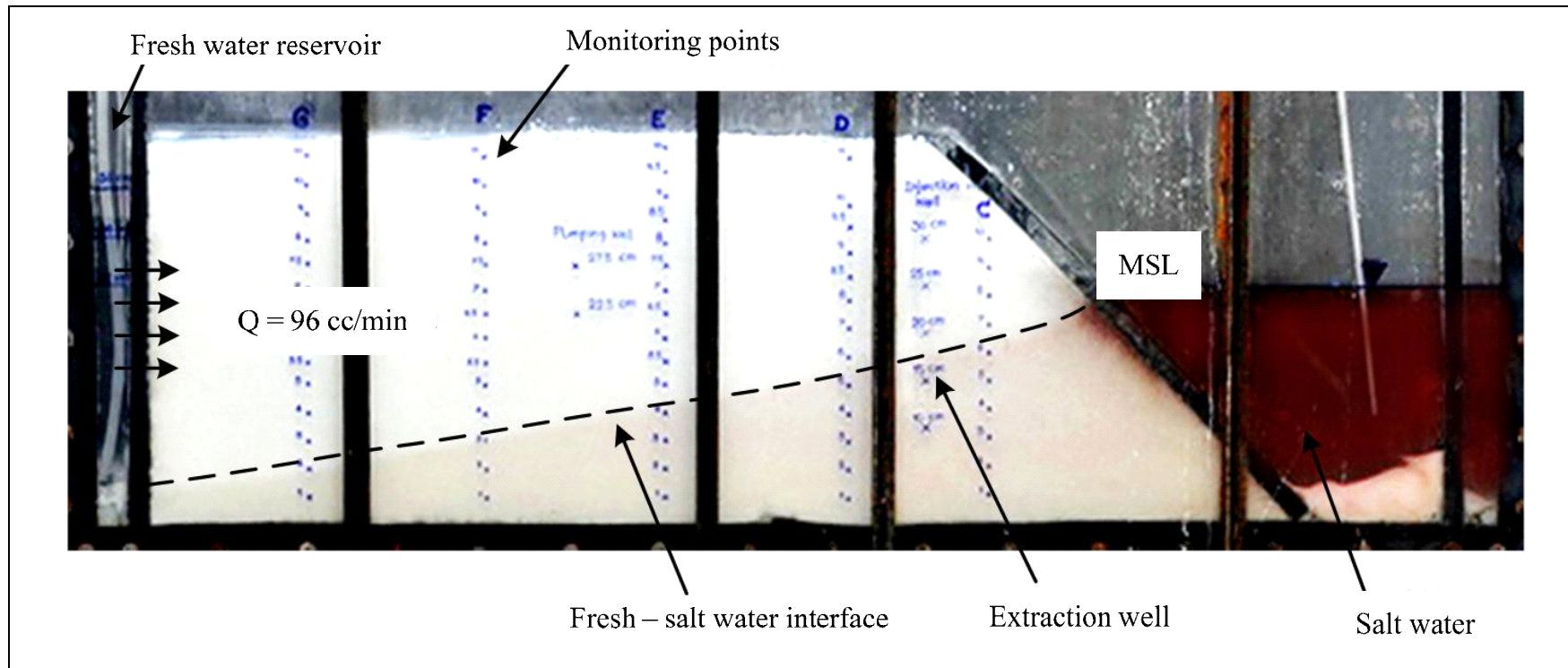


**Figure 5.5** Dye testing for salt water extraction at - 10 cm (10 cm below MSL) with  $Q_{SE} = 50$  cc/min

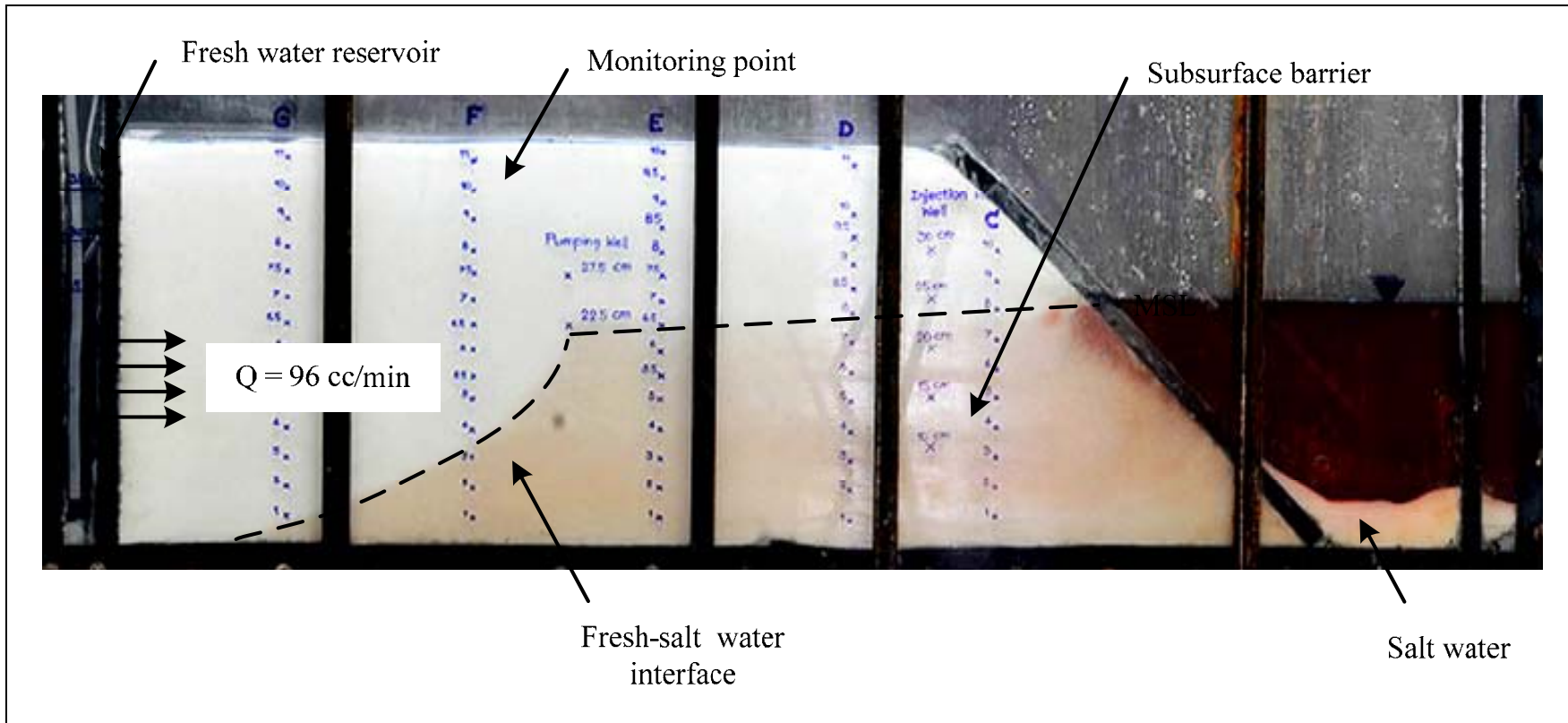


**Figure 5.6** Dye testing for subsurface barrier at  $D_B = -10 \text{ cm}$  (10 cm below MSL)

# **CHAPTER VI**

## **DISCUSSIONS AND CONCLUSIONS AND RECOMMENDATIONS FOR FUTURE STUDIES**

### **6.1 Discussions and Conclusions**

The movements of fresh-salt water interface in unconfined aquifer near shoreline are simulated using a physical model in the laboratory. The results indicate that under natural dynamic equilibrium condition between the discharge of fresh water and salt water intrusion, the salinity measurements agree reasonably well with the mathematical solution given by Ghyben-Herzberg. Fresh water pumping (usage) from the aquifer notably moves the fresh-salt water interface toward the well, depending on the pumping rates and the difference between the far-field recharge (fresh water reservoir) and salt water levels ( $\Delta h$ ). To control the movement of the interface the fresh water injection near the shoreline is more favorable than salt water extraction. The fresh water injection rate of about 10% of the discharge rate at the well can effectively push the interface toward the shoreline, and keeping the pumping water free of salinity. The effectiveness of the subsurface barrier technique depends heavily on the depth of the barrier below the salt water level. The barrier depth that is equivalent to  $\Delta h$  can effectively keep the interface below that obtained from the condition of fresh water pumping without the barrier.

It is recognized that the two dimensional flow in unconfined aquifer assumed here may not truly represent the actual conditions in many areas. The results obtained

from these simplified conditions are useful to qualitatively determine the effectiveness of the controlling methods. The conclusions drawn above are based purely on the simulation results. In actual practice however the selection and suitability of each method depends on site-specific conditions. Subsurface barrier requires high initial investment on geotechnical work but has an advantage over other methods in terms of the long-term maintenance. Fresh water injection needs continuous supply of surface fresh water which may not be available near some coastal areas. The salt water extraction technique consumes continuous energy even though its performance is proved effective.

## **6.2 Recommendations for future studies**

The study in this research can be taken as a preliminary guideline and process of study and design of controlling methods for the salt water intrusion. More laboratory testing should be performed using unconfined aquifer with different thickness. Confined aquifers can also be simulated under various discharge and recharge rates and pressures.

## REFERENCES

- Aharmouch, A., and Larabi. A. (2001), Numerical Modeling of Saltwater Interface Upconing in Coastal Aquifers. **First International Conference on Saltwater Intrusion and Coastal Aquifers-Monitoring.**
- Bear J., Zhou, Q. and Bensabat, J. (2001), Three Dimensional Simulation of Seawater Intrusion in Heterogeneous Aquifers, with Application to the Coastal Aquifer of Israel. **First International Conference on Saltwater Intrusion and Coastal Aquifers-Monitoring.**
- Cooper, H. H. et al (1964). Sea Water in Coastal Aquifers. **U.S. Geological Survey Water Supply Paper** 1613-C. 84 pp.
- Demirel, Z. (2003). The history and evaluation of saltwater intrusion into a coastal aquifer in mersin, Turkey. **Journal of environmental management**, Vol. 70 : 275-282
- Elhassadi, A. (2007). Sea water intrusion in Derna located in the Green mountain region, Libya- a threatening recurrent phenomenon calling for desalination. **Desalination**, Vol. 220 : 189-193
- Fang, H. Y. (1997). **Introduction to Environment Geotechnology**. (pp. 448-450). USA: CRC Press LLC.
- Freeze, R. A. and Cherry, J. A. (1979). **Groundwater**. (pp. 375-379).USA: Prentice Hall, Inc.

- Giambastiani, B. M. S., Antonellini, M., Essink, G. H. P. O. and Stuurman, R. J. (2007). Saltwater intrusion in the unconfined coastal aquifer of Ravenna (Italy) : A numerical model. **Journal of Hydrology**, Vol. 340 : 91-104
- Henry, H. R. (1960). Salt water Intrusion into Coastal Aquifers,” **Intern. Assoc. Hydrol**, Publ.52, pp. 478-487.
- Hubbert, M. K. (1940). The theory of ground-water motion, **Jour. Geol.**,Vol. 48 : 785-944
- Johnson, T. (2007), Battling Seawater Intrusion in the Central & West Coast Basins, *WRD Technical Bulletin. Volextraction seams to be feasible to all site conditions*. This technique however consumes high enerume 13.
- Kohout, F. A. (1960a). Cyclic flow of saltwater in the Biscayne aquifer of southeastern Florida, **Journal of Geophysical Research** 65(7), 2133-2141
- Kohout, F. A. (1960b). Flow pattern of fresh and salt water in the Biscayne aquifer of the Miami area, Florida: **International Association of Scientific Hydrology**. 52:. 440-448
- Kouzana, L., Mammou, A. B. and Felfoul, M. S. (2007). Seawater intrusion and associated processes : case of the Korba aquifer (Cap-Bon, Tunisia). **C.R. Geoscience**, Vol. 341 : 21-35
- Lee, R. F. and Cheng L.(1974). A comparative study of lipids of water-striders from marine, estuarine, and freshwater environments; Halobates, Rheumatobates, Gerris (Heteroptera : Gerridae). **Limnology and. Oceanography**. 19 : 958-965

- Lookjan, A., Chalermyanont T. and Arrykul, S. (2009), Three-dimensional density-dependent seawater intrusion modeling for the hat yai basin. **The 14<sup>th</sup> National convention on civil engineering, Suranaree University of Technology.** Page: 1253-1259.
- Milnes, E. and Renard, P. (2003). The problem of salt recycling and seawater intrusion in coastal irrigated plains : an example from the Kiti aquifer (Southern Cyprus). **Journal of Hydrology**, Vol. 288 : 327-343
- Narayan, K. A., Schleeberger, C. and Bristow, K. L. (2007). Modeling seawater intrusion in the Burdekin Delta irrigation area, North Queensland, Australia. **Agricultural water management**, Vol. 89 : 217-228
- Nguyen, A. D., Savenije, H. H. G. and Pham, D. N. and Tang, D. T. (2007). Using salt intrusion measurements to determine the freshwater discharge distribution over the branches of a multi-channel estuary : The Mekong Delta case. **Estuarine coastal and shelf science**, Vol. 77 : 433-455
- Pinder, G. F. and Cooper H. H. (1970). A numerical technique for calculating the transient position of the saltwater front, **Water Resource Research**, 6(3) : 875-82
- Segol, G. and Pinder, G. F. (1976). Transient simulation of saltwater intrusion in southeastern Florida, **Water Resources Research**, V.12, no 1, pp. 65-70
- Todd, D. K. and Mays, L. W. (2005). **Groundwater Hydrology**. 3<sup>rd</sup> Edition (pp. 589-606).USA: John Wiley and Sons, Inc.

**APPENDIX A**

**TECHNICAL PUBLICATION**

## **TECHNICAL PUBLICATION**

Weingchanda, P. and Fuenkajorn, K., 2010. **Laboratory simulations of seawater intrusion and controlling methods**, In the EIT-JSCE Joint Symposium on Engineering for Geo-Hazards: Earthquakes and Landslides-for surface and subsurface Structure, Imperial Queen's Park Hotel, Bangkok, Thailand, 6-8 September 2010. PP.1-8.

## Laboratory simulations of seawater intrusion and controlling methods

P. Weingchanda & K. Fuenkajorn

*Geomechanics Research Unit, Suranaree University of Technology, Thailand*

**Keywords:** Seawater intrusion, physical model, salinity, fluid flow

**ABSTRACT:** Physical scaled-down model has been used to simulate salt water intrusion into unconfined aquifer near shoreline. The results indicate that under natural dynamic equilibrium between the discharge of fresh water and salt water intrusion the location of fresh-salt water interface agree reasonably well with the mathematical solution of Ghyben-Herzberg. Fresh water pumping (usage) from the aquifer notably move the fresh-salt water interface toward the pumping well, depending on the pumping rates and the difference between the far-field recharge (fresh water reservoir) and salt water level ( $\Delta h$ ). Controlling the salt water intrusion by fresh water injection near the shoreline is more favorable than the salt water extraction. The fresh water injection rate of about 10% of the discharge rate can effectively push the interface toward the shoreline, and keeping the pumping water free of salinity. The effectiveness of subsurface barrier technique depends heavily on the depth of the barrier below the salt water level. The barrier depth that is equivalent to  $\Delta h$  can effectively keep the interface below the pumping well.

### 1 INTRODUCTION

Seawater intrusion or encroachment is the movement of salt water from the ocean into coastal aquifers (Todd & Mays, 2005). The problem of seawater intrusion has occurred in many cities that are located on and relied upon near-shore aquifers. This problem has become increasingly more severe as the coastal population increases. The rise of sea levels due to the global warming, and the increasing demands of fresh water from the industries have recently contributed to the seawater intrusion problem. Several controlling methods have been proposed and implemented to minimize the seawater intrusion. These include the applications of salt water extraction wells, injection of fresh water and subsurface barrier (Johnson, 2007; Brian & Kevin, 2002). Performance of these methods has been assessed by a variety of numerical models, as well as by in-situ monitoring and measurements. Selection criteria for the suitable methods depend primarily on the geology of the near-shore aquifers, water usage, availability of the materials, and economic constraints. Extensive studies have been carried out to understand the mechanisms of the seawater intrusion, particularly via numerical simulations (Bear, 2001; Aharmouch & Larabi, 2001). Explicit observations and performance assessment of these controlling methods have however been rare.

The objectives of this research are to simulate the seawater intrusion into unconfined aquifers and to assess the efficiency of the controlling methods by using scaled-down physical models in the laboratory. The simulated conditions include the dynamic equilibrium between the salt water and fresh water under the natural condition, the impact of fresh water pumping, the performance of salt water extraction, fresh water injection and subsurface barrier. The results of this research reveal the efficiency of the controlling methods and improve our understanding of the seawater intrusion mechanisms. Accuracy and validity of the Ghyben-Herzberg relation will also be verified.

## 2 PHYSICAL MODEL

Figure 1 shows the test frame used in this study. It is fabricated by two 1.6×1.6 m wide with 1.5 cm thick clear acrylic plates set 1.5 cm apart. They are water-tightly secured in upright position during the test. The gap between the two plates is filled with test materials (sorted sand). Desired thickness of the overburden, salt water depth, and fresh water level can be obtained by pre-calculating the material volume. The left edge is open to allow adding fresh water. The salt water is stored in the right reservoir. The pumping depth locations are simulated by using series of drilled holes as shown in the figure.

## 3 TEST METHOD

Clean sorted sand (0.6-0.8 mm) is used to simulate the unconfined aquifer. The aquifer is 40 cm high and 140 cm long. Figure 2 shows the positions of monitoring points on the rear acrylic plate. These points are used to measure the salinity of the fluid circulating in the model under various test conditions. A fresh water reservoir is located on the left side of the frame, while the saturated brine reservoir (prepared to simulate the seawater) with lower heads is located on the right. Two head differences are used ( $\Delta h=5$  and 10 cm) and are maintained constant during each test series (Figure 1). Here the brine is maintained 100% saturated during the test. It is prepared by mixing distilled water with pure sodium chloride. There are numeral outlet holes drilled on the back of the clear acrylic sheet, and hence allowing withdrawals of the fluid samples at various depths and locations of the aquifer. The changes of the water salinity at various points can therefore be monitored as a function of time. All test series are performed under room (ambient) temperature.

## 4 GHYBEN-HERZBERG RELATION

Recognizing the approximations inherent in the Ghyben-Herzberg relation, more exact solutions for the shape of the interface have been developed from potential flow theory (Todd & May, 2005).

$$z^2 = \frac{2\rho q x}{\Delta\rho K} + \left( \frac{\rho q}{\Delta\rho K} \right)^2 \quad (1)$$

where  $x$  is distance from shoreline,  $z$  is the distance from mean sea level to interface,  $\Delta\rho=\rho_s - \rho_f$  ( $=0.23 \text{ g/cm}^3$ ),  $K$  is the hydraulic conductivity of the unconfined aquifer ( $=0.35 \text{ cm/s}$ ) and  $q$  is the fresh water flow per unit length of shoreline.

The corresponding shape of the water table is given by

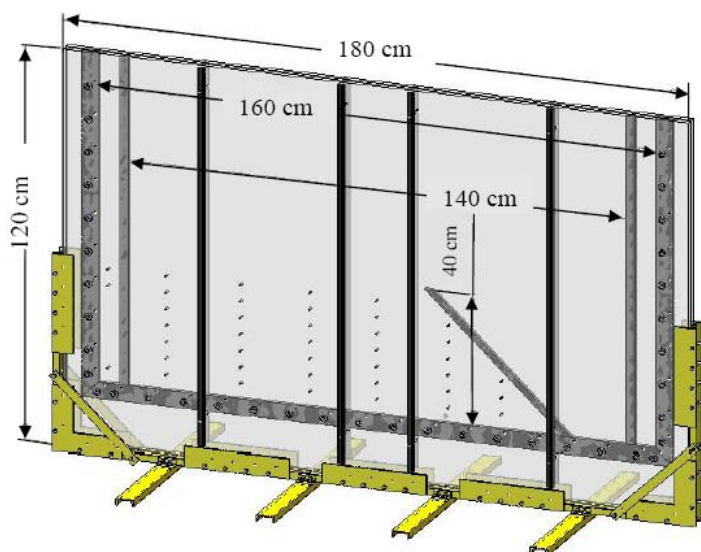


Figure 1. Test frame used to simulate salt water intrusion.

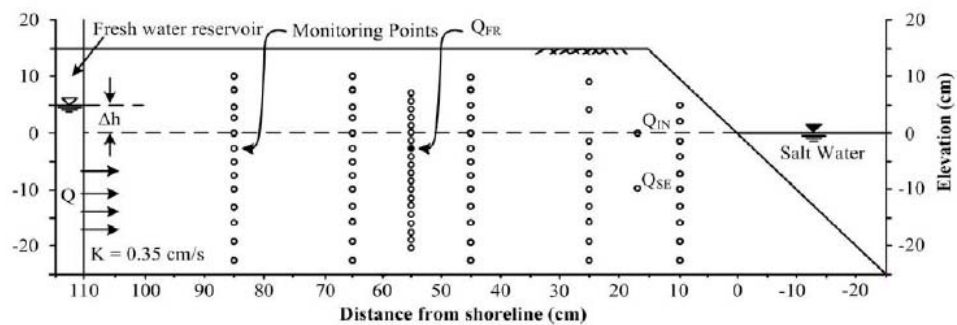


Figure 2. Test parameters and locations of monitoring points on acrylic sheets.

$$h_f = \left( \frac{2\Delta\rho qx}{(\rho + \Delta\rho)K} \right)^{1/2} \quad (2)$$

The width  $x_0$  of the submarine zone through which fresh water discharges into the sea can be obtained for  $z=0$ , yielding

$$x_0 = \frac{\rho q}{2\Delta\rho K} \quad (3)$$

The depth of the interface beneath the shoreline is defined as.

$$z_0 = \frac{\rho q}{\Delta\rho K} \quad (4)$$

From the above equations for  $\Delta h=10$  cm,  $x_0=5.09$  cm, and for  $\Delta h=5$  cm,  $x_0=1.94$  cm. The fresh water pumping (usage) is simulated by withdrawing the water at the depth of 2.5 cm below the simulated mean sea level (MSL).

## 5 TEST RESULTS

The hydraulic conductivity of the sorted sand simulating the aquifer is determined by the Darcy test method as 0.35 cm/s. Under natural condition (no pumping and extraction wells) the fresh-salt water interface observed from the physical model agrees well with that calculated by the widely known Ghyben-Herzberg equation (Todd & Mays, 2005) for both  $\Delta h=5$  cm and 10 cm. Comparison of the interface profiles obtained from the test and from the solution for  $\Delta h=10$  cm is given in Figure 3.

The results indicate that the fresh-salt water interface moves toward the pumping location. The lower  $\Delta h$  value shows a shallower interface, as the interface move toward the pumping well. For  $\Delta h = 5$  cm with 30 and 70 cc/min the fresh-salt water interfaces move 95-110 cm from the shoreline. The pumped water however remains fresh as long as the pumping rate ( $Q_{FR}$ ) is less than about 50% of the discharge inflow rate,  $Q$  (see Table 1). At a higher pumping rate the up-coning characteristics of the interface will occur, and eventually increasing the salinity of the pumping well (Figures 4 and 5).

Figure 6 shows some results of the fresh water injection at the rate  $Q_{IN}$  of 7 and 50 cc/min. The injection depth is at the MSL. This technique seems to be the most effective method compared to the other two methods. The salt water extraction (Figure 7) is effective only when the extraction rate ( $Q_{SE}$ ) is greater than the water usage ( $Q_{FR}$ ).

The subsurface barrier is simulated by creating a vertical zone near the shoreline with a permeability about half of the sand aquifer. The results suggest that there is an optimum barrier depth that can reduce the salinity of the water usage well. The shallow barrier (-5 cm below MSL) can keep the pumping water well fresh by reducing the flow of the fresh water into the sea and hence raising the groundwater table above those obtained from the pumping condition. The deep barrier (-15 cm below MSL) can also keep the water well fresh by minimizing the intrusion of the sea water at depth above the impermeable layer. However for the intermediate barrier depth of -10 cm below MSL, this method can not keep the pumping water well fresh (Figure 8).

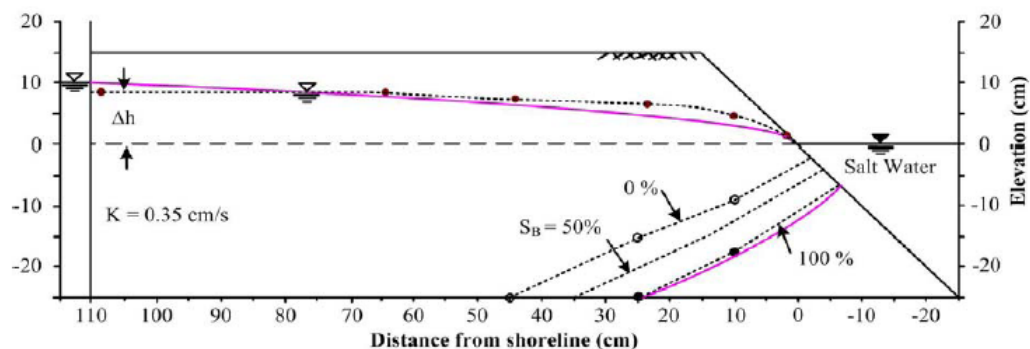


Figure 3. Simulations of natural condition (dash lines) and compared with the Ghyben-Herzberg solution (solid lines).

Table 1. Test parameters and results.

Testing series	Test Parameters						Results		
	$\Delta h$ (cm)	Q (cc/min)	$Q_{FR}$ (cc/min)	$Q_{SE}$ (cc/min)	$Q_{IN}$ (cc/min)	$D_B$ (cm)	% salinity of pumping well	1 *	2 *
Natural condition	10	62						-	-
	5	24						-	-
Water pumping	10	62	0.2				0	<-25	<-25
		85	10				0	<-25	-22
		120	100				0	-23	-14
	5	25	5				0	-13	-11
		50	30				20	-10	-9
		96	70				45	-8	-7
Salt water Extraction	5	75		15			20	-8	-5
		100	70	50			0	-15	-10
		150		100			0	-22	-13
Fresh water Injection	5	80			7			-18	-10
		80	70		15		0	-19	-11
		57			50			-23	-15
Sub-surface barrier	5	96	70			-5	0	-17	-9
						-10	15	-11	-7
						-15	0	-15	-8

1\* Elevations of fresh-salt water interface at pumping location (cm)

2\* Elevations of fresh-salt water interface at half distance between shoreline and pumping location (cm)

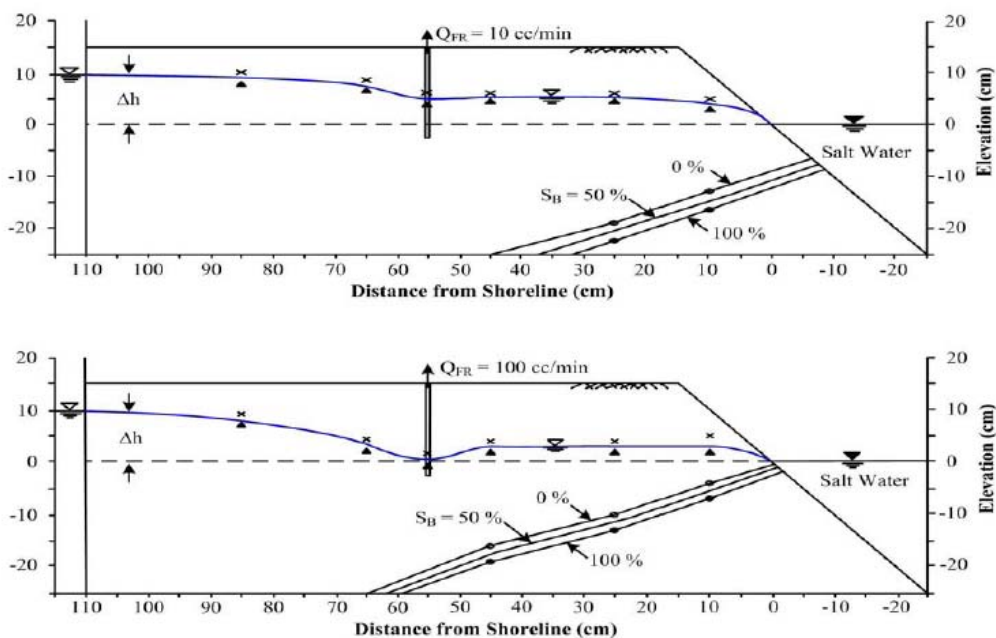


Figure 4. Simulations of water pumping at  $\Delta h=10$  cm,  $Q_{FR}=10$  cc/min (top),  $Q_{FR}=100$  cc/min (bottom).

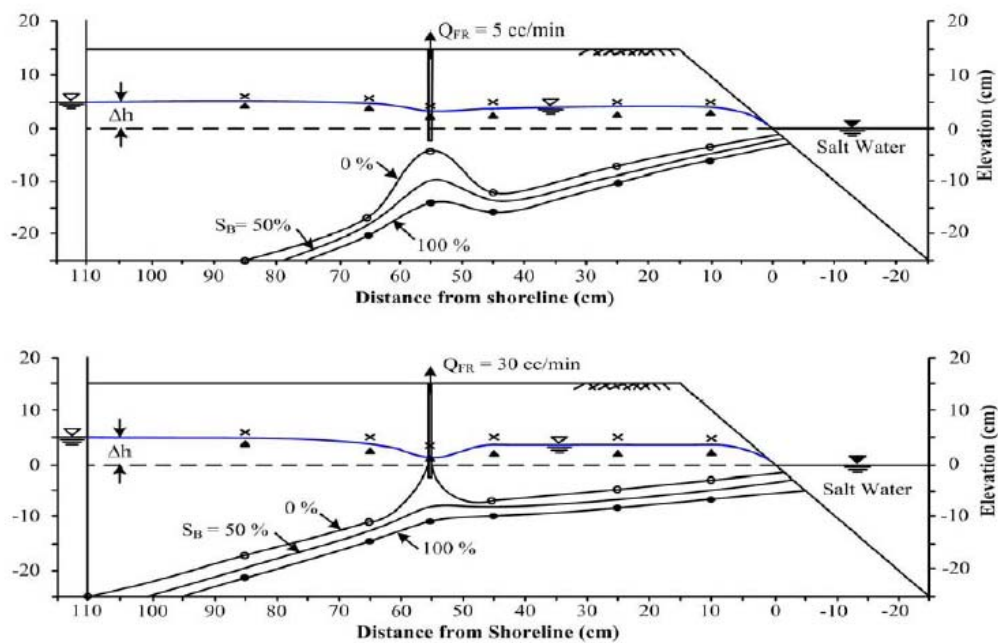


Figure 5. Simulations of water pumping at  $\Delta h=5$  cm,  $Q_{FR}=5$  cc/min (top),  $Q_{FR}=30$  cc/min (bottom).

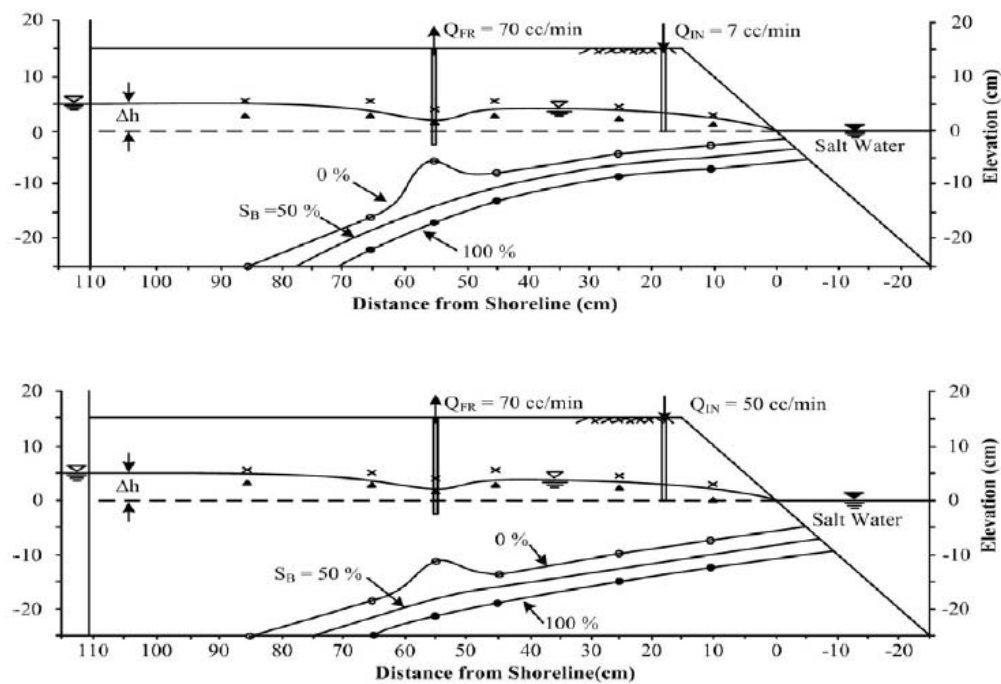


Figure 6. Simulations of fresh water injection at MSL,  $Q_{IN}=7$  cc/min (top),  $Q_{IN}=50$  cc/min (bottom).

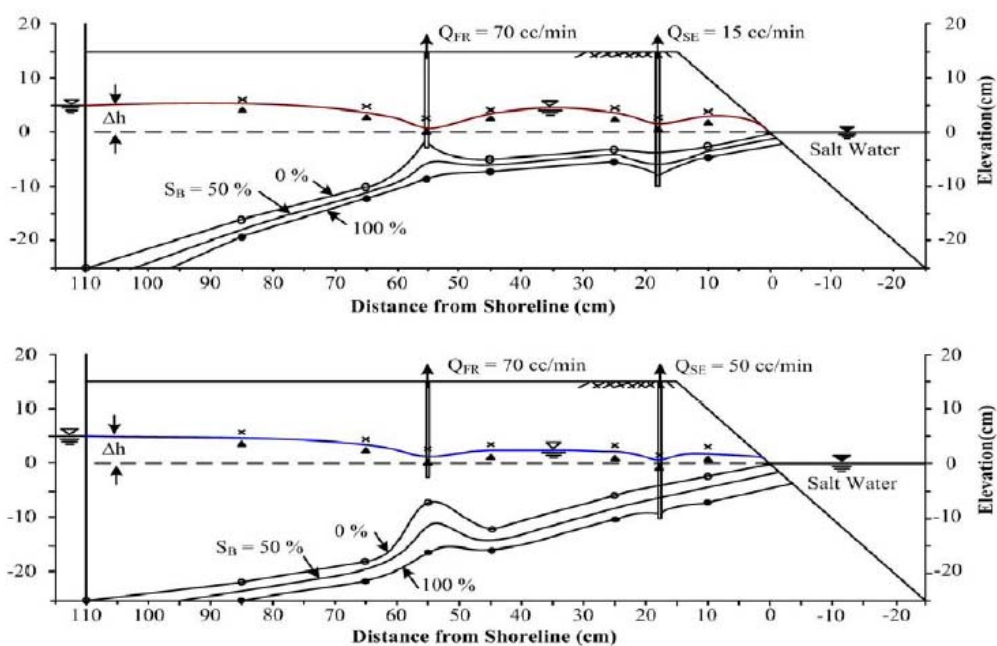


Figure 7. Simulations of salt water extraction at -10 cm,  $Q_{SE} = 15$  cc/min (top),  $Q_{SE} = 50$  cc/min (bottom).

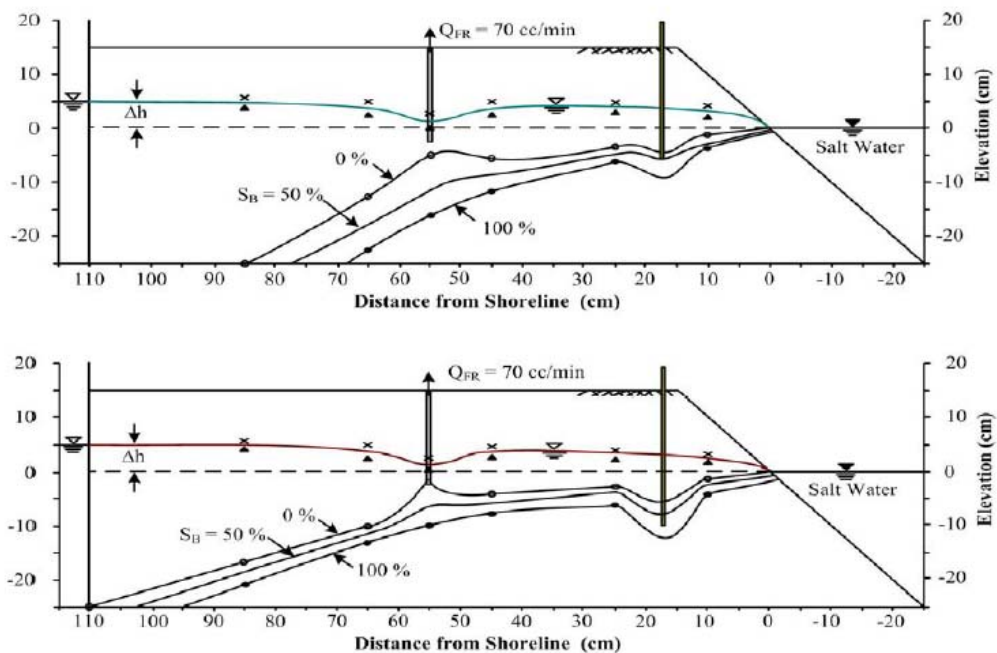


Figure 8. Simulations of at subsurface barrier at  $D_B = -5$  cm (top),  $D_B = -10$  cm (bottom).

## 6 DISCUSSIONS AND CONCLUSIONS

The movements of fresh-salt water interface in unconfined aquifer near shoreline are simulated in this study. The results indicate that under natural dynamic equilibrium between the discharge of fresh water and salt water intrusion the salinity measurements agree reasonably well with the solution given by Ghyben-Herzberg. Fresh water pumping (usage) notably move the fresh-salt water interface toward the well, depending on the pumping rates and the difference between the far-field discharge (fresh water reservoir) and salt water level ( $\Delta h$ ). Fresh water injection near the shoreline is more favorable than salt water extraction. The fresh water injection rate of about 10% of the discharge rate can effectively push the interface toward the shoreline, and keeping the pumping water free of salinity. The effectiveness of subsurface barrier technique depends heavily on the depth of the barrier below the salt water level. The barrier depth that is equivalent to  $\Delta h$  can effectively press the interface lower.

It is recognized that the two dimensional flow in unconfined aquifer assumed here may not truly represent the actual conditions in many areas. The results obtained from these simplified conditions are useful to qualitatively determine the effectiveness of the controlling methods. The conclusions drawn above are based purely on the simulation results. In actual practice however the selection and suitability of each method depends on site-specific conditions. Subsurface barrier requires high initial investment on geotechnical work but has an advantage over other methods in terms of the long-term maintenance. Fresh water injection needs continuous supply of surface fresh water which may not be available near coast lines. Salt water pumps the intruded salt water and hence lowers the interface.

### ACKNOWLEDGEMENT

This research is funded by Suranaree University of Technology. Permission to publish this paper is gratefully acknowledged.

### REFERENCES

- Todd D K, and Mays L W, (2005), *Groundwater Hydrology*. 3<sup>rd</sup> Edition (pp. 589-606).USA: John Wiley and Sons, Inc.
- Johnson T, (2007), Battling Seawater Intrusion in the Central & West Coast Basins, *WRD Technical Bulletin. Volextraction seams to be feasible to all site conditions*. This technique however consumes high enerume 13.
- Brian D E, and Kevin R E, (2002), Saltwater Intrusion in Los Angeles Area Coastal Aquifers-the Marine Connection, U.S. *Geological Survey*, Edited by James W. Hendley II and Peter H. Stauffer.
- Aharmouch A and Larabi A, (2001), Numerical Modeling of Saltwater Interface Upconing in Coastal Aquifers. *First International Conference on Saltwater Intrusion and Coastal Aquifers-Monitoring*.
- Bear J, Zhou Q and Bensabat J, (2001), Three Dimentional Simulation of Seawater Intrusion in Heterogeneous Aquifers, with Application to the Coastal Aquifer of Israel. *First International Conference on Saltwater Intrusion and Coastal Aquifers-Monitoring*.

## **BIOGRAPHY**

Miss. Pajeeraporn Weingchanda was born on September 27, 1984 in Khonkean province, Thailand. She received her Bachelor's Degree in Engineering (Geotechnology) from Suranaree University of Technology in 2007. For her post-graduate, she continued to the Master's degree in Geological Engineering Program, Institute of Engineering, Suranaree University of Technology. During graduation, 2007-2010, she was a research assistant at the Geomechanics Research Unit, Suranaree University of Technology. She published technical paper related to environment science, titled **“Laboratory simulations of seawater intrusion and controlling methods”** In the EIT-JSCE Joint Symposium on Engineering for Geo-Hazards: Earthquakes and Landslides-for surface and subsurface Structure, Imperial Queen's Park Hotel, Bangkok, Thailand, 6-8 September 2010. PP 1-8.